

Larry Wilding

[Handwritten scribbles]

*Jim Colver -
Soil Survey Quality
Assurance Staff
USFC*

**UNITED STATES DEPARTMENT OF AGRICULTURE
SOIL CONSERVATION SERVICE**

**160 East 7th Street
CHESTER, PA 19013**

SUBJECT: Soils - Geophysical Investigations in Jamaica; 10 to 20 January 1994
DATE: 1 March 1994

TO: Dr. Larry Wilding
Department of Soil and Crop Sciences
College of Agriculture and Life Sciences
Texas A & M University
College Station, Texas 77843-2474

PURPOSE:
To explore the potential of using ground-penetrating radar (GPR) and electromagnetic induction (EM) techniques to assess the short-range variability of soils and soil properties in areas of restored bauxite lands.

PARTICIPANTS:
Jim Doolittle, Soil Specialist, SCS, Chester, PA
Wendy Greenberg, Graduate Student, Texas A & M University, College Station, TX
Dr. Larry Wilding, Professor, Texas A & M University, College Station, TX

ACTIVITIES:
I arrived in Mandeville, Jamaica, on 10 January 1994. The geophysical equipment arrived in Kingston, Jamaica, on 5 January 1994, but did not clear customs until 14 January. Field studies were conducted at four sites near Mandeville on January 15 to 19, 1994. I returned to Philadelphia, Pennsylvania, on January 20, 1994.

EQUIPMENT:
The electromagnetic induction meter used in this study was the EM38 manufactured by Geonics Limited*. This meter is portable and requires only one person to operate. Principles of operation have been described by McNeill (1). The depth of penetration is dependent upon the intercoil spacing, transmission frequency, and coil orientation relative to the ground surface. The EM38 meter integrates values of apparent conductivity over the upper 0.75 m of

* Use of trade names in this report is for identification purposes only and does not constitute endorsement by the authors or their institutions.

1. McNeill, J. D. 1986. Geonics EM38 ground conductivity meter, operating instructions and survey interpretation techniques. Technical Note TN-21. Geonics Limited, Mississauga, Ontario. pp. 27.

the soil profile in the horizontal dipole orientation, and over the upper 1.5 m of the soil profile in the vertical dipole orientation.

The radar units used was the Subsurface Interface Radar (SIR) System-8 manufactured by Geophysical Survey Systems, Inc. * The SIR System-8 consists of the Model 4800 control unit, the ADTEK SR 8004H graphic recorder, the Model 38 video display unit, a SONY model TCD-D3 digital tape-corder, a power distribution unit, a 30 meter (m) transmission cable and antennas. The Model 3110 (120 mHz) and the Model 3102 (500 mHz) antennas were used in this survey. The system was powered by a 12-volt vehicular battery. The use and operation of GPR have been discussed by Morey (2), Doolittle (3), and Daniels and others (4).

SURVEY SITES:

The four research areas are referred to as the Battersea, Martin Hill, Russell Place, and Trinity sites. Figure 1 is a topographic map of the Battersea Site (18°04'19" N, 77°29'36" W). This moderately-steep to steep, restored mined-out site has been stabilized with improved grasses. Relief was about 15.8 m. Soils at this site were members of the Typic and Lithic Udorthents subgroups. The location of one subsite is shown in Figure 1.

Figure 2 is a topographic map of the Martin Hill Site (18°05'42" N, 77°30'20" W). This nearly level to gently sloping site has not been mined and is presently in pasture. Relief was about 4.0 m. Soils at this site were members of the Typic and Lithic Eutrudox subgroups. The locations of the two subsites are shown in Figure 2. Subsite A was located near a farm road which formed the northern boundary of the site. Within this subsite, relief was about 2.0 m. Subsite B was located in a nearly level area in the southern portion of the site. Within this subsite, relief was about 0.4 m.

* Use of trade names in this report is for identification purposes only and does not constitute endorsement by the authors or their institutions.

2. Morey, R. M. 1974. Continuous subsurface profiling by impulse radar. pp. 212-232. In: Proceedings, ASCE Engineering Foundation Conference on Subsurface Exploration for Underground Excavations and Heavy Construction, held at Henniker, New Hampshire. Aug. 11-16, 1974.

3. Doolittle, J. A. 1987. Using ground-penetrating radar to increase the quality and efficiency of soil surveys. pp. 11-32. In: Reybold, W. U. and G. W. Peterson (eds.) Soil Survey Techniques, Soil Science Society of America. Special Publication No. 20. p. 98

4. Daniels, D. J., D. J. Gunton, and H. F. Scott. 1988. Introduction to subsurface radar. IEE Proceedings 135:(F4) 278-320.

Figure 3 is a topographic map of the Russell Place Site ($18^{\circ}03'44''$ N, $77^{\circ}28'31''$ W). This moderately-steep to steep, restored mined-out site has been stabilized with improved grasses. Relief was about 15.8 m. Soils at this site were members of the Typic and Lithic Udorthents subgroups. The locations of the two subsite are shown in Figure 3. Subsite A was located on an upper side-slope in an area which adjoined a farm road. Within this subsite relief was about 1.5 m. Subsite B was located on a lower-lying foot slope. Within this subsite relief was about 1.3 m.

Figure 4 is a topographic map of the Trinity Site ($18^{\circ}02'12''$ N, $77^{\circ}25'54''$ W). This moderately-steep, recently restored site had sparse vegetative cover. Runoff had resulted in conspicuous gully erosion. Relief was about 15.3 m. Soils at this site were members of the Typic and Lithic Udorthents subgroups. The locations of the two subsite are shown in Figure 4. Both subsites were located on side-slopes. Relief was about 2.9 m and 2.6 m within subsites A and B, respectively.

FIELD METHODS:

Relatively coarse grids were set up at the four research sites. The grid interval was 15 m. Wooden stakes were inserted into the ground at each grid intersection. This provided 30, 20, 25, and 30 observation points (coarse grid intersections) at the Battersea, Martin Hill, Russell Place and Trinity sites, respectively. A transit was used to establish grid lines and determine surface elevations at each grid intersection. At each grid intersection, measurements were obtained with the EM38 meter in both the horizontal and vertical dipole orientations. In addition, a GPR survey was conducted along parallel, north-south trending, 15 m grid lines at the Martin Hill Site.

Each site contained two plots or subsites. These subsites were named Plot A and Plot B. With the exception of the Battersea site, coarse grids were established at each site which included each of the two research plots and a portion of the surrounding area. At the Battersea site, only one research plot was included in the coarse grid.

Detail grids were set up across a portion of each subsite within the four research sites. The grid interval was one meter. A transit was used to establish grid lines and determine surface elevations at each grid intersection. Grids varied in size ranging from 56 to 120 m². At each grid intersection, measurements were obtained with the EM38 meter in both the horizontal and vertical dipole orientations. With the exception of the Battersea site, GPR surveys were completed across portions of each subsite.

GROUND-PENETRATING RADAR

Background:

Ground-penetrating radar techniques have been used to map bauxite

reserves (5) and stratigraphic features (6) in Jamaica. In these studies, GPR provided exceptional profiles of soil/bedrock contacts and delta-reef complexes. In bauxite deposits, the maximum depth of observation (with an 80 MHz antenna) was about 9 m (5). In the study conducted by Benson and Yuhr (5), GPR techniques were used to assess bauxite reserves, to aid mine and restoration planning, haul road and drag-line placement, and to reduce stripping.

Calibration:

Calibration trials were conducted at each site using different scanning times and antennas. The objectives of these trials were to determine the dielectric constant and velocity of propagation of electromagnetic energy through soils, establish the depth scale, optimize control and recording settings, and select the most suitable antenna.

During calibration trials, multiple traverses were conducted with both the 120 MHz and 500 MHz antennas. Soil depth considerations and the resolution of subsurface features influenced the selection of scanning times and antennas. Both antennas provided adequate depths of observation. Scanning time varied from 60 to 120 nanoseconds (ns). A scanning rate of 25.6 scans/sec was used in these trials and in all subsequent field work. Both antennas discerned planar reflectors (such as soil horizons and geologic strata) and point reflectors (such as rock fragments and buried artifacts).

The velocity of propagation and depth scales were estimated based on known depths to buried reflectors (buried paint cans). The reflectors, buried at depths of 46 to 56 cm, were clearly distinguishable on radar profiles. In Figure 5, the reflection (hyperbolic pattern) from a buried paint can be seen to the immediate left of "A" at a depth of 46 cm. This profile was recorded using a 500 MHz antenna with a scanning time of 60 ns.

At each site, based on a known depth to a buried reflector, the depth of observation and the velocity of propagation were estimated. Velocity of propagation varied from 0.065 to 0.087 m/ns. These velocities were faster than those (0.026 to 0.035 m/ns) obtained in the deeper investigations of Benson and Yuhr (5). Differences were attributed to shallower observation depths and varying soils and

5. Benson, R. and L. Yuhr. 1992. Assessment of bauxite reserves using ground penetrating radar. p. 229-336. IN: P. Hanninen and S. Autio (ed.) Fourth International Conference on Ground Penetrating Radar. Geological Survey of Finland, Special Paper 16. June 8-13, 1992. Rovaniemi, Finland. pp. 365.

6. Forgotson, J. M., J. D. Pigott, and J. D. Skinner. 1990. Ground penetrating radar imaging of sequence boundaries and lithofacies variations in a mixed siliciclastic carbonate depositional sequence. p. 34. IN: Olhoeft, G. R., J. E. Lucius, and D. L. Wright (ed.) Third International Conference on Ground-Penetrating Radar. May 14-18, 1990. Lakewood, Colorado. pp. 88.

moisture contents. The dielectric constant of the examined soil materials ranged from 12 to 21.

The 500 MHz antenna was used in areas of restored soil materials having predominantly shallow (0 to 50 cm) and moderately deep (50 to 100 cm) depths to bedrock. Benson and Yuhr (5) reported that the 500 MHz antenna would provide a maximum observation depth of about 1.5 m. Our studies revealed the potential of obtaining observation depths greater than 2.6 m in fine-textured soils with the 500 MHz antenna. In undisturbed areas having greater anticipated depths to bedrock, the 120 MHz antenna was used with an observation depth of about 3.85 m. In most areas, greater depths could have been attained with this antenna.

Interpretations:

Ground-penetrating radar detects but does not identify subsurface features. The identification of subsurface features is based on knowledge, field experience, and interpretative skills. The purpose of the radar surveys were to determine the thickness of restored soil materials and the depth to limestone bedrock. The detection and identification of the soil/bedrock interface often depended upon local soil conditions, the depth, geometry, and composition of the bedrock surface, and the presence of scattering bodies within the soil.

Figure 6 is a processed profile from an undisturbed area at the Martin Hill Site. Processing was limited to horizontal scaling, customizing color transform and color tables, and annotations. The scale along the left-hand border of the radar profile represents depth and is in meters. The radar traverse was conducted in an area of very deep (>1.5 m), fine-textured soils. Soils were members of the Typic Eutrudox subgroup.

The amount of energy reflected back to an antenna from a subsurface interface is a function of the dielectric gradient existing between the adjoining materials. The greater or more abrupt the difference in dielectric properties, the greater the amount of energy reflected back to the antenna, and the more intense will be the amplitude of the image recorded on the radar profile. In Figure 6, the abrupt upper boundary of an oxic horizon forms the first major subsurface interface. Generally, the upper part of the oxic horizon was noticeably firmer than the overlying surface layers. In the lower part of the radar profile (Figure 6), two prominent features (inferred to be pinnacles of limestone bedrock) are apparent. Variations in the amplitude of the bedrock surface were presumed to reflect differences in form and degree of induration or weathering.

In areas of restored soils, radar profiles were often more difficult to interpret. Figure 7 and 8 are processed radar profiles from an area of restored soil materials at the Russell Place Site. Processing was limited to horizontal scaling, customizing color transform and color tables, and annotations. The scales along the left-hand borders of these profiles represents depth and are in meters. These radar traverses were conducted on a lower-lying foot

slope area of moderately deep to very deep, fine-textured restored soils. Soils were members of the Typic Udorthents subgroup.

In figures 7 and 8, the complex stratigraphy of restored areas having moderately deep to very deep soils are evident. In Figure 7, the bedrock surface extends across the lower part of this profile and ranges in depth from about 70 cm to 300 cm. Several subsurface interfaces occur in the upper part of this profile. In the absence of ground-truth observations, the identities of these layers were unknown. They were presumed to represent successive layers of restored soil materials. In Figure 7, most portions of the radar profile between depths of 1.0 to 2.5 m lack subsurface reflections. This portion of the profile was presumed to consist of relatively homogeneous materials which lacked contrasting layers.

In areas of restored soils, the correct identification of the bedrock surface was undoubtedly not always achieved. Typically, radar profiles contained reflections from layers of restored soil materials, rock fragments, bedrock surface and lithologic facies. The underlying limestone bedrock varied laterally in degrees of weathering and vertically in composition. On some radar profiles, reflections from the bedrock surface were poorly expressed and partially masked by rock fragments and discontinuous soil strata.

In Figure 8 the imagery is more complex. This profile was obtained along a parallel grid line spaced only 4 meters upslope from the radar profile shown Figure 7. In Figure 8, multiple subsurface reflections from bedding and fracture planes within the bedrock and layers of restored soil materials complicate interpretations. A segmented line has been used to identify the interpreted bedrock surface. This surface appears to be highly variable over short distances and ranges in depth from about 105 cm to 185 cm.

The radar detects but does not identify interfaces. In areas of restored soils, where subsurface layers are numerous or segmented, a large number of ground-truth verification pits and auger observations are required to satisfactorily interpret the radar profiles.

Results:

Figure 9 contains three-dimensional surface net diagrams of the soil surface (A) and the bedrock surface (B) within the Martin Hill Site. These plots were prepared from transit and GPR data collected at 20 observation points (grid intersections). The plot of the soil surface was prepared from the data collected with the transit. The bedrock surface plot was prepared by subtracting, at each observation point, the interpreted depth to bedrock (from the radar profiles) from the measured elevation of the soil surface. In each plot, the contour interval is 0.5 m. Vertical exaggeration is 2.5.

Data used to construct computer simulations in this report were kriged and the resulting matrices were smoothed using cubic spline techniques. The data sets used to construct Figure 9 and similar simulations of the larger grids were small (20 to 30 observation points), the distance between observation points relatively large (15

m) and the survey area relatively large (0.27 to 0.45 ha). Because of these factors, the simulation of the bedrock surface in Figure 9B is considered overly simplified and lacks sufficient detail for an area of karst.

Figure 10 is a two-dimensional plot of the depth to bedrock within the Martin Hill Site. Generally, in the southern and northeastern portions of this site, soils were shallow and moderately deep to bedrock. In the northwestern portion of this site, soils were very deep to bedrock. At this site, no relationship was found to exist between the elevation of the soil surface and the depth to bedrock. The depth to bedrock can not be predicted from landscape position alone.

Based on 20 observations, the depth to bedrock within the Martin Hill Site averaged 1.2 m and ranged from about 0.5 to 3.4 m. The distribution of depths to bedrock by 0.5 m soil depth classes is shown in Figure 11. The soils at this site were predominantly moderately deep (65%). Areas of deep (15%) and very deep (20%) soils formed a distinct trough in the northwest portion of this site (see Figure 10).

Figure 12 contains three-dimensional surface net diagrams of the soil surface (A) and the bedrock surface (B) within Subsite A of the Martin Hill Site. In each plot, the contour interval is 0.5 m. In each diagram, the vertical exaggeration is 2.5. These plots were prepared from transit and GPR data collected at the 128 observation points (grid intersections). Ridges and furrows are evident in the plot of the soil surface (Figure 12A). The topography of the bedrock surface is highly variable, suggests the occurrence of solution features, and can not be predicted from the topography of the soil surface. Within this subsite, an extremely weak (or no) relationship ($r^2 = 0.023$) was found to exist between the elevation of the soil surface and the depth to bedrock.

Two-dimensional plots of the soil surface (A) and the depth to bedrock (B) within Subsite A of the Martin Hill Site are shown in Figure 13. In most areas of this subsite, depths to bedrock are variable over short distances and appear to reflect the effects of dissolution. A limestone pinnacle and funnel depression are suggested by the contour patterns in the lower left-hand and upper right-hand corners of Figure 13B, respectively.

Based on 128 observations, the depth to bedrock within Subsite A of the Martin Hill Site averaged 2.91 m and ranged from 0.6 to 3.85 m. Depths exceeded 3.85 m at several observation points, but were not recorded. Though deeper depths could have been achieved, the maximum observation depth was set at 3.85 m on the GPR's control unit. The distribution of depths to bedrock by 0.5 m soil depth classes is shown in Figure 14 (upper). The soils at this subsite were predominantly very deep (87%). Areas of moderately deep (4%) and deep (9%) soils were located in the extreme southeastern part of the subsite (see Figure 13B, lower right-hand corner).

Figure 15 contains three-dimensional surface net diagrams of the soil surface (A) and the bedrock surface (B) within Subsite B of the Martin Hill Site. In each plot, the contour interval is 0.5 m. In each diagram, the vertical exaggeration is 2.5. These plots were prepared from transit and GPR data collected at 128 observation points (grid intersections). Once again, ridges and furrows are evident in the plot of the soil surface (Figure 15A). The bedrock surface (Figure 15B) appears to be highly pitted with solution features. However, compared with Subsite A, depths to bedrock are shallower and the topography of the bedrock surface is less variable. At this site, a very weak relationship ($r^2 = 0.117$) was found to exist between the elevation of the soil surface and the depth to bedrock.

Two-dimensional plots of the soil surface (A) and the depth to bedrock (B) within Subsite B of the Martin Hill Site are shown in Figure 16. Generally, depths to bedrock are fairly uniform across this subsite. Depths become more variable in the right-hand portion of the subsite where several features which suggest funnel depressions are evident. The topography of the bedrock surface (Figure 16B) can not be predicted from the topography of the soil surface (Figure 16A).

Based on 128 observations, the depth to bedrock within Subsite B of the Martin Hill Site averaged 0.63 m and ranged from 0.47 to 1.46 m. The distribution of depths to bedrock within Subsite B by 0.5 m soil depth classes is shown in Figure 14 (lower). The soils at this subsite were predominantly moderately deep (72%) and shallow (22%). Areas of deep (6%) soils were located in the extreme eastern part of the subsite (see Figure 16B, right-hand margin).

Figure 17 contains three-dimensional surface net diagrams of the soil surface (A) and the bedrock surface (B) within Subsite A of the Russell Place Site. In each plot the contour interval is 0.5 m. In each diagram, the vertical exaggeration is 2.5. These plots were prepared from transit and GPR data collected at the 80 observation points (grid intersections). Subsite A was located on an upper side-slope (see Figure 3). The topography of the soil and bedrock surfaces are similar. However, the topography of bedrock surface is more pronounced. This relationship reflects the smoothing effect of a relatively thin mantle of restored soil materials over a bedrock surface.

Two-dimensional plots of the soil surface (A) and the depth to bedrock (B) within Subsite A of the Russell Place Site are shown in Figure 18. Generally, depths to bedrock are shallow to moderately deep and relatively invariable (< 0.5 m) across this subsite. Based on 80 observations, the depth to bedrock within Subsite A of the Russell Place Site averaged 0.63 m and ranged from about 0.46 to 0.92 m. The distribution of depths to bedrock by 0.5 m soil depth classes is shown in Figure 19 (upper). The soils at this subsite were moderately deep (89%) and shallow (11%).

Figure 20 contains three-dimensional surface net diagrams of the soil surface (A) and the bedrock surface (B) within Subsite B of the Russell Place Site. In each plot, the contour interval is 0.5 m. In each diagram, the vertical exaggeration is 2.5. These plots were prepared from transit and GPR data collected at 72 observation points (grid intersections). This subsite was located on a lower-lying foot slope. Compared with Subsite A, depths to bedrock were deeper and the topography of the bedrock surface was more variable at Subsite B. However, at each subsite there was a similar, weak relationship between elevation and depth to bedrock (r^2 0.23 and 0.22 at Subsides A and B, respectively).

Two-dimensional plots of the soil surface (A) and the depth to bedrock (B) within Subsite B of the Russell Place Site are shown in Figure 21. Generally, depths to bedrock are variable across the subsite. Depths to bedrock were greater and more variable over short distances in the left-hand portion of the subsite where a rather deep trough in the bedrock surface is evident (Figure 21B). The topography of the bedrock surface (Figure 21B) can not be predicted from the topography of the soil surface (Figure 21A).

Based on 72 observations, the depth to bedrock within Subsite B of the Russell Place Site averaged 1.58 m and ranged from 0.70 to 3.85 m. Depths exceeded 3.85 m at several observation points, but were not recorded. Though deeper depths could have been achieved, the maximum observation depth was set at 3.85 m on the GPR's control unit. The distribution of depths to bedrock within Subsite B by 0.5 m soil depth classes is shown in Figure 19 (lower). The soils at this subsite were deep (50%), very deep (34%), and moderately deep (16%).

Figure 22 contains three-dimensional surface net diagrams of the soil surface (A) and the bedrock surface (B) within Subsite A of the Trinity Site. In each plot the contour interval is 0.5 m. These plots have not been vertically exaggerated. This subsite was located on a side-slope (see Figure 4). These plots were prepared from transit and GPR data collected at the 80 observation points (every 2 m by 1 m grid intersection). The topography of the soil and bedrock surfaces were similar. However, the topography of bedrock surface was more pronounced.

Two-dimensional plots of the soil surface (A) and the depth to bedrock (B) within Subsite A of the Trinity Site are shown in Figure 23. Generally, depths to bedrock were relatively invariable (< 0.6 m) across this subsite. This pattern reflects a rather uniform cover of restored soil materials over a smoothed bedrock surface.

Based on 80 observations, the depth to bedrock within Subsite A of the Trinity Site averaged 0.51 m and ranged from about 0.30 to 0.88 m. The distribution of depths to bedrock by 0.5 m soil depth classes is shown in Figure 24 (upper). The soils at this subsite were shallow (80%) and moderately deep (20%).

Figure 25 contains three-dimensional surface net diagrams of the soil surface (A) and the bedrock surface (B) within Subsite B of the Trinity Site. In each plot, the contour interval is 0.5 m. This subsite was located on a side-slope (see Figure 4). These plots have not been vertically exaggerated. These plots were prepared from transit and GPR data collected at 80 observation points (every 2 m by 1 m grid intersection). Depths to and the topography of the bedrock surface are similar to those of Subsite A. At each subsite there was a extremely weak relationship between elevation and depth to bedrock (r^2 0.101 and 0.049 at Subsites A and B, respectively).

Two-dimensional plots of the soil surface (A) and the depth to bedrock (B) within Subsite B of the Trinity Site are shown in Figure 26. Generally, depths to bedrock were relatively invariable (< 0.6 m) across the subsite.

Based on 80 observations, the depth to bedrock within Subsite B of the Trinity Site averaged 0.42 m and ranged from 0.23 to 0.80 m. The distribution of depths to bedrock within Subsite B by 0.5 m soil depth classes is shown in Figure 24 (lower). The soils at this subsite were shallow (80%) and moderately deep (20%).

ELECTROMAGNETIC INDUCTION

Background:

Electromagnetic induction techniques were used by Benson and Yuhr (5) to map bauxite reserves in Jamaica. In their project, a Geonics EM31 meter was used to measure the apparent conductivity of earthen materials to a depth of about 6.0 m. Benson and Yuhr reported that values of apparent conductivity were low and ranged from 4 to 7 mS/m. Only minor lateral variations in EM responses were noted across the surveyed areas. These authors observed values of less than 3.5 mS/m where limestone bedrock was at or near the surface; 3 to 4 mS/m where limestone bedrock was at depths of 1.5 to 3 m; and values greater than 4 mS/m where the limestone bedrock was at depths greater than 3 m.

Electromagnetic induction is an imperfect geophysical tool and is not equally suitable for use in all soil investigations. The success of an EM survey depends on the nature and variability of soil properties. Electromagnetic induction methods have been most effective in areas where subsurface soil properties are fairly homogeneous, the effects of one factor dominant over the others, and variations in the EM response can be related to changes in a single factor (e.g. volumetric moisture, soluble salt content, clay content, soil depth, or mineralogy). These parameters would not be satisfied in the present survey.

Calibration:

Prescribed operating procedures were followed at each subsite (1). At each grid intersection, the EM38 meter was placed on the ground surface and measurements were taken in both the horizontal and vertical dipole orientations. Final inphase nulling was performed when the meter was placed on the ground surface and after the meter was reorientated. At all survey sites, soils displayed very low conductivities and considerable magnetic susceptibility. McNeill (1) noted that, in areas of high magnetic susceptibility and when the meter is calibrated at a height of 1.5 m,

"the signal from the susceptibility causes a positive meter deflection in the vertical mode (when the Mode switch is in the I/P position) and a negative meter deflection in the horizontal dipole mode."

At low conductivities (< 30 mS/m) the EM38 meter is very responsive to metallic objects (cultural noise) and sensitive to electrical interference from cultural or atmospheric sources. At each site, these problems affected survey results. Magnetic susceptibility was exceptional high at the Trinity Site. At this site, exceedingly low or negative values were often recorded in the vertical dipole orientation.

Computer Simulations:

Electromagnetic induction meters provide limited vertical resolution and depth information. However, as discussed by Benson and others (7), the absolute values are not necessarily diagnostic in themselves, but lateral and vertical variations in these measurements are significant. Interpretations of the EM data are based on the identification of spatial patterns in the data set appearing on two-dimensional contour plots.

Electromagnetic induction methods focuses on the rate and magnitude of change in EM response from place to place. Isarithmic maps prepared from EM data can provide a graphic description of variations in soils and/or soil properties within survey areas.

Figures 27 to 40 represents two-dimensional isarithmic maps prepared from data collected with the EM38 meter. These simulations chart apparent conductivity values collected in the horizontal and the vertical dipole orientations. In preparing the isarithmic maps of the study sites and subsites, it was hoped that these diagrams would provide a comprehensive maps of soils and the depth to bedrock.

1. McNeill, J. D. 1986. Geonics EM38 ground conductivity meter, operating instructions and survey interpretation techniques. Technical Note TN-21. Geonics Limited, Mississauga, Ontario. pp. 27.

7. Benson, R. C., R. A. Glaccum, and M. R. Noel. 1984. Geophysical techniques for sensing buried wastes and waste migration: an application review. IN: D. M. Nielsen and M. Curls (eds.) Surface and Borehole Geophysical Methods in Ground Water Investigations. NWWA/EPA Conference, San Antonio, Texas. p. 533-566.

Results:

In the present study, an attempt was made to use a Geonics EM38 meter to assess the depth to bedrock in areas of restored soils. Depths to bedrock were determined from a limited number of soil pits and interpretations from radar profiles. Obviously, this procedure was subject to several sources of errors (positioning, interpretative, point versus integrated area measurements).

Figures 27 and 28 represent two-dimensional isarithmic maps prepared from data collected at the Battersea Site with the EM38 meter in the horizontal and the vertical dipole orientations, respectively. These simulations were prepared from data collected at 30 observation sites. Values of apparent conductivity varied less than 4 mS/m across this site. This range is small and well within the range of observation errors. At this site, in the horizontal dipole orientation, apparent conductivity averaged 3.38 mS/m with values ranging from 1.5 to 5.0 mS/m. In the vertical dipole orientation, the apparent conductivity averaged 2.53 mS/m with values ranging from 1.2 to 5.1 mS/m. At 90 percent of the observation sites, values of apparent conductivity decreased with increasing observation depth. Generally, in the horizontal dipole orientation, values of apparent conductivity increased with decreasing elevation (see Figure 1). However, this relationship was very weak ($r^2 = 0.153$).

Figures 29 and 30 represent two-dimensional isarithmic maps prepared from data collected at 20 observation sites within the Martin Hill Site. The anomalous patterns in the upper part of Figures 29 and 30 and the lower right-hand corner of Figure 30 were produced by unusually high apparent conductivity values recorded at singular observation points. The relative size of these patterns reflect, in part, the coarseness of the grid interval. These anomalous values are believed to reflect interference from buried metallic objects or adjoining metallic fences.

At the Martin Hill Site, in the horizontal dipole orientation, apparent conductivity averaged 1.67 mS/m with values ranging from 0.4 to 10.2 mS/m. In the vertical dipole orientation, apparent conductivity averaged 0.92 mS/m with values ranging from 0.2 to 3.9 mS/m. At 90 percent of the observation sites, values of apparent conductivity decreased with increasing observation depth. A weak relationship was observed between the depth to bedrock and the EM response in the horizontal orientation ($r^2 = 0.29$). No relationships were found to exist between surface elevations and EM responses (see Figure 2).

Figure 31 represents two-dimensional isarithmic maps prepared from data collected at 96 observation sites within Subsite A of the Martin Hill Site. Values of apparent were higher at this subsite than within other portions of the Martin Hill Site. Higher responses were attributed to differences in management practices and interference from a metallic fence.

At Subsite A, in the horizontal dipole orientation, apparent conductivity averaged 5.66 mS/m with values ranging from 1.1 to 11.5

mS/m. In the vertical dipole orientation, apparent conductivity averaged 4.28 mS/m with values ranging from 1.6 to 10.1 mS/m. At 72 percent of the observation sites, values of apparent conductivity decreased with increasing observation depth. A weak relationship was observed between surface elevation and the EM response in the horizontal orientation ($r^2 = 0.277$). No relationships were found to exist between depths to bedrock and values of apparent conductivity.

Figure 32 represents two-dimensional isarithmic maps prepared from data collected at 40 observation sites within Subsite B of the Martin Hill Site. At this subsite, in the horizontal dipole orientation, apparent conductivity averaged 2.29 mS/m with values ranging from 0.5 to 5.5 mS/m. In the vertical dipole orientation, apparent conductivity averaged 1.76 mS/m with values ranging from 0.5 to 3.2 mS/m. At 70 percent of the observation sites, values of apparent conductivity decreased with increasing observation depth. No relationships were observed between surface elevations or depths to bedrock and EM responses.

Figures 33 and 34 represent two-dimensional isarithmic maps prepared from data collected at 25 observation sites within the Russell Place Site. At this site, in the horizontal dipole orientation, apparent conductivity averaged 4.03 mS/m with values ranging from 1.0 to 8.6 mS/m. In the vertical dipole orientation, apparent conductivity averaged 2.9 mS/m with values ranging from 0.7 to 7.6 mS/m. At 92 percent of the observation sites, values of apparent conductivity decreased with increasing observation depth. No relationships were observed between elevations of the soil surface and EM responses.

Figure 35 represents two-dimensional isarithmic maps prepared from data collected at 40 observation sites within Subsite A of the Russell Place Site. Values of apparent were higher at this subsite than within other portions of the Russell Place Site. Higher responses were attributed to differences in management practices and interference from a metallic fence.

At Subsite A, in the horizontal dipole orientation, apparent conductivity averaged 4.24 mS/m with values ranging from 0.2 to 19.2 mS/m. In the vertical dipole orientation, apparent conductivity averaged 3.19 mS/m with values ranging from 0.7 to 21.3 mS/m. At 75 percent of the observation sites, values of apparent conductivity decreased with increasing observation depth. No relationships were observed between surface elevations or depths to bedrock and values of apparent conductivity.

Figure 36 represents two-dimensional isarithmic maps prepared from data collected at 25 observation sites within Subsite B of the Russell Place Site. At this subsite, in the horizontal dipole orientation, apparent conductivity averaged 4.44 mS/m with values ranging from 1.2 to 7.9 mS/m. In the vertical dipole orientation, apparent conductivity averaged 2.98 mS/m with values ranging from 1.0 to 8.0 mS/m. At 92 percent of the observation sites, values of apparent conductivity decreased with increasing observation depth. Weak relationships were observed between the depth to bedrock and the

EM response in the horizontal ($r^2 = 0.169$) and vertical dipole ($r^2 = 0.335$) orientations. No relationships were found to exist between surface elevations and values of apparent conductivity.

Figures 37 and 38 represent two-dimensional isarithmic maps prepared from data collected at 29 observation sites within the Trinity Site. At this site, in the horizontal dipole orientation, apparent conductivity averaged 5.06 mS/m with values ranging from 0.7 to 11.4 mS/m. In the vertical dipole orientation, apparent conductivity averaged 1.35 mS/m with values ranging from -2.2 to 6.0 mS/m. At 93 percent of the observation sites, values of apparent conductivity decreased with increasing observation depth. Weak relationships were observed between surface elevations and the EM responses in the horizontal ($r^2 = 0.158$) and vertical dipole ($r^2 = 0.363$) orientations.

Figure 39 represents two-dimensional isarithmic maps prepared from data collected at 40 observation sites within Subsite A of the Trinity Site. At this subsite, in the horizontal dipole orientation, apparent conductivity averaged 4.23 mS/m with values ranging from 2.5 to 6.2 mS/m. In the vertical dipole orientation, apparent conductivity averaged 0.79 mS/m with values ranging from -2.6 to 3.9 mS/m. At all observation sites, values of apparent conductivity decreased with increasing observation depth. At this subsite, no relationships were observed between surface elevations or depths to bedrock and EM responses.

Figure 40 represents two-dimensional isarithmic maps prepared from data collected at 40 observation sites within Subsite B of the Trinity Site. At this subsite, in the horizontal dipole orientation, apparent conductivity averaged 4.64 mS/m with values ranging from 0.7 to 10.1 mS/m. In the vertical dipole orientation, apparent conductivity averaged 0.86 mS/m with values ranging from -1.9 to 3.8 mS/m. At 88 percent of the observation sites, values of apparent conductivity decreased with increasing observation depth. A weak relationship was observed between surface elevations and EM responses in the horizontal ($r^2 = 0.394$). No relationships were found to exist between depths to bedrock and values of apparent conductivity.

RESULTS:

1. The performance of ground-penetrating radar (GPR) was most exceptional. This study represented my first opportunity to use GPR on highly-weathered tropical soils. In the profiled fine-textured tropical soils, observation depths were greater than 3 meters (even with the 500 MHz antenna). Generally, in nontropical areas, profiling depths in fine-textured soils are less than 0.5 to 1.0 meters. This study confirms feelings that GPR technology is well suited to use in highly weathered tropical soils having low electrical conductivities.
2. In areas of restored soils, radar profiles were often difficult to interpret because of intricate and discontinuous subsurface layers

and numerous rock fragments. These features produced complicated radar profiles and, in some areas, masked the soil/bedrock interface. In the absence of sufficient ground-truth observations, the identities of many layers were unknown.

3. At selected sites and subsites, depth to bedrock could not be predicted from landscape position alone. However, across most sites general trends could be predicted. At Russell Place, a lower-lying foot slopes site had deeper depths to bedrock than a higher-lying side slopes site. At the Trinity Site, two side-slope sites had similar depths to bedrock.

4. Electromagnetic induction is an imperfect geophysical tool and is not equally suitable for use in all soil investigations. The success of an EM survey depends on the nature and variability of soils and soil properties. Electromagnetic induction methods have been most effective in areas where subsurface soil properties are fairly homogeneous, the effects of one factor dominant over the others, and variations in the EM response can be related to changes in a single factor (e.g. soil moisture, soluble salt content, clay content, soil depth, or mineralogy). These parameters were not satisfied in areas of restored soils.

The use of the EM38 meter to assess the depth to bedrock in areas of restored mined-out bauxite lands appears to be inappropriate. At each site, no to very weak relationships (r^2 ranged from 0.002 to 0.335) were found between EM response and the depth to bedrock or elevation. The EM31 meter may be a more appropriate tool.

At the four sites, values of apparent conductivity were exceedingly low and no marked conductivity contrasts (either vertical or lateral) were observed. In the horizontal dipole orientation, the EM responses averaged 4.38 mS/m with a range of 0.2 to 19.2 mS/m. In the vertical dipole orientation, the EM response averaged 1.85 mS/m with a range of -2.60 to 21.3 mS/m. **

At several sites, anomalous values were recorded. These anomalies were believed to represent the presence of cultural features. EM techniques are influenced by cultural features such as building, wires, fences, buried metallic objects and responses to differences in management (i.e. applications of irrigation waters and fertilizers). It is believed that many of the anomalous patterns appearing in the accompanying diagrams are related to "cultural noise."

At 83 percent of the observation points (385), values of apparent conductivity were greater in measurements taken in the horizontal dipole orientation (0 to 0.75 m) than in vertical dipole orientation

** The negative values in the vertical dipole orientation can not be explained. Simon Boniwell of Geonics believes that it could be due to calibration or operator errors; Lynn Yuhr of Technos suspects an influence magnetic susceptibility.

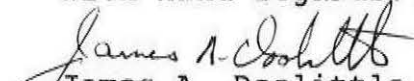
(0 to 1.5 m). This pattern of decreasing apparent conductivity values with depth conforms with the anticipated soil conductivity model. This model hypothesized that more conductive materials (restored soil materials) would occur near the surface and more resistive materials would occur with increasing soil depths (limestone bedrock). However, the apparent contrast between these two materials was less than anticipated. In terms of apparent conductivity, the electrical properties of restored soil materials and the limestone bedrock were closely similar.

5. Electromagnetic techniques produce qualitative results. Results depend on the adequacy of interpretations. Interpretations are based on available information concerning the nature and complexity of soil, geologic, and terrain conditions at a site, and the number and type of observations used to support or verify the inferences drawn from EM survey.

6. A disc containing this MS Word file and a Lotus worksheet file has been included with the trip report sent to Dr. Wilding.

I appreciated the opportunity to work in the field with Ms. Wendy Greenberg and Dr. Larry Wilding. They have become good friends and I shall always warmly remember our shared experiences in Jamaica. I can only hope that I have provided some measure of assistance to them.

With kind regards,


James A. Doolittle
Soil Specialist

cc:

J. Culver, National Leader, SSQAS, NSSC, SCS, Lincoln,
A. Dornbusch, Jr., Director, MWNTC, SCS, Lincoln, NE
C. S. Holzhey, Assistant Director, NSSC, SCS, Lincoln, NE

Ground-Penetrating Radar

Ground-penetrating radar (GPR) has been used as a pedologic tool in the United States since 1978. The National Cooperative Soil Survey Program has used GPR to assess properties of soils which affect their use, management, and classification. Principal uses have been to estimate the variability and taxonomic composition of soils, chart the lateral extent and estimate the depth and thickness of soil horizons, geologic layers, and peat, and map soils.

The presence, depth, and lateral extent of soil horizons are used to classify soils and estimate the taxonomic composition of soil map units. Most diagnostic subsurface horizons (Soil Survey Staff, 1992) used to classify soils within the United States have been charted with GPR. These horizons often have abrupt upper boundaries which contrast from overlying horizons in physical (texture, bulk density, moisture) and chemical (organic carbon, calcium carbonate, sesquioxide contents) properties. Typically, these interfaces produce strong reflections and distinct GPR imagery.

Ground-penetrating radar techniques have been used to estimate depths to soil horizons (Collins and Doolittle, 1987; Doolittle, 1987), hard pans (Olson and Doolittle, 1985), dense till (Collins et al., 1989), and permafrost (Doolittle et al., 1990b and 1992); infer soil color or organic carbon content (Doolittle, 1982; Collins and Doolittle, 1987); determine thickness and profile the depths of organic soil materials (Shih and Doolittle, 1984; Doolittle, 1983; Collins et al., 1986; and Doolittle et al., 1990a); chart the depths to relatively shallow (< 12 m) water tables in predominantly coarse textured soils (Shih et al., 1986); assess the concentration of lamellae in soils (Farrish et al., 1990; Mokma et al., 1990); and evaluate the thickness of surface (Doolittle, 1987) and active layers (Doolittle et al. 1990b). Interpretations have been used to update soil survey reports (Doolittle, 1982 and 1987; Schellentrager and Doolittle, 1985; Collins et al., 1986; Schellentrager et al., 1988; and Puckett et al., 1990). In addition, GPR has been used to study changes in soil properties which affect forest productivity (Farrish et al., 1990) and stress in citrus trees (Shih et al., 1985).

Ground-penetrating radar is an impulse radar system designed for shallow, subsurface investigations. This system operates by transmitting short pulses of electromagnetic energy into the ground from an antenna. Each pulse consists of a spectrum of frequencies distributed around the center frequency of the transmitting antenna. Whenever a pulse contacts an interface separating layers of differing electromagnetic properties, a portion of the energy is reflected back to the receiving antenna. The receiving unit amplifies and samples the reflected energy and converts it into a similarly shaped waveform in a lower frequency range. The processed reflected waveforms are displayed on a graphic recorder or are recorded on magnetic tape for future playback and/or processing.

The GPR is a time scaled system. This system measures the time that it takes for electromagnetic energy to travel from the antenna to an interface (e.g. soil horizon, stratigraphic layer) and back. In order to convert the travel time into a depth scale, either the velocity of pulse propagation or the depth to a reflector must be known. The relationship among depth (d), two-way, pulse travel time (t), and velocity of propagation (v) are described by the following relationship:

$$v = 2d/t$$

The velocity of propagation is principally effected by the dielectric constant (e) of the profiled material(s) according to the equation:

$$e = (c/v)^2$$

where c is the velocity of propagation in a vacuum (0.3 m/ns). The amount and physical state (temperature) of water in the soil profile have the greatest effect on the dielectric constant.

The GPR does not perform equally in all soils. The maximum probing depth of GPR is, to a large degree, determined by the conductivity of the soil. Soils having high electrical conductivities rapidly dissipate the radar's energy and restrict observation depths. The principal factors influencing the conductivity of soils to electromagnetic radiation are: (i) degree of water saturation, (ii) amount and type of salts in solution, and (iii) the amount and type of clay.

Electromagnetic conductivity is essentially an electrolytic process which takes place through moisture filled pores. As water-filled porosity is increased, the velocity of signal propagation is reduced and the rate of signal attenuation is increased. As the degree of water saturation increases, the observation depth of the radar is restricted.

Electrical conductivity is directly related to the concentration of dissolved salts in the soil solution. Ions absorbed to clay particles can undergo exchange reactions with ions in the soil solution and thereby contribute to the electrical conductivity of the soil. The concentration of ions in the soil solution is dependent upon the clay minerals present, the pH of the soil solution, the degree of water filled porosity, the nature of the ions in solution, and the relative proportion of ions on exchange sites.

Soil texture (clay content) and mineralogy strongly influence the performance of GPR. The maximum observation depth of GPR increases as the clay content decreases and the proportion of low activity clays increases. Generally, observation depths are 5 to 25 meters in coarse textured soils, 2 to 5 meters in moderately-coarse textured soils, 1 to 2 meters in moderately-fine textured soils, and less than 0.5 to 1.5 meters in fine textured soils. As discussed earlier, these observation depths become less as the concentration of soluble salts in solution and the exchange activities of clays increase.

Smectitic and vermiculitic clays have higher cation-exchange capacities than kaolinitic and oxidic (e.g. gibbsite and goethite) clays, and under similar soil moisture conditions, are more conductive.

References

- Collins, M. E., and J. A. Doolittle. 1987. Using ground-penetrating radar to study soil microvariability. *Soil Sci Soc. Am. J.* 51:491-493.
- Collins, M. E., J. A. Doolittle, and R. V. Rourke. 1989. Mapping depth to bedrock on a glaciated landscape with ground-penetrating radar. *Soil Science Society of America J.* 53:1806-1812.
- Collins, M. E., G. W. Schellentrager, J. A. Doolittle, and S. F. Shih. 1986. Using ground-penetrating radar to study changes in soil map unit composition in selected Histosols. *Soil Science Society of America J.* 50:408-412.
- Doolittle, J. A. 1982. Characterizing soil map units with the ground-penetrating radar. *Soil Survey Horizons* 22(4):3-10.
- Doolittle, J. A. 1983. Investigating Histosols with ground-penetrating radar. *Soil Survey Horizons* 23(3):23-28.
- Doolittle, J. A. 1987. Using ground-penetrating radar to increase the quality and efficiency of soil surveys. IN *Soil Survey Techniques*, Soil Science Society of America Special Publ. No 20. pp. 11-32.
- Doolittle, J. , P. Fletcher, and J. Turenne. 1990a. Estimating the thickness and volume of organic materials in cranberry bogs. *Soil Survey Horizons* 31(3)73-78.
- Doolittle, J. A., M. A. Hardisky, and S. Black. 1992. A ground-penetrating radar study of Goodream Palsas, Newfoundland, Canada. *Arctic and Alpine Research* 24(2):173-178.
- Doolittle, J. A., M. A. Hardisky, and M. F. Gross. 1990b. A ground-penetrating radar study of active layer thicknesses in areas of moist sedge and wet sedge tundra near Bethel, Alaska, U.S.A. *Arctic and Alpine Research* 22(2):175-182.
- Farrish, K. W., J. A. Doolittle, and E. E. Gamble., 1990. Loamy substrata and forest productivity of sandy glacial drift soils in Michigan. *Canadian Journal of Soil Science* 70:181-187.
- Mokma, D. L., R. J. Schaetzl, E. P. Johnson, and J. A. Doolittle. 1990. Assessing Bt horizon character in sandy soils using ground-penetrating radar: Implications for soil surveys. *Soil Survey Horizons.* 30(2):1-8.

Olson, C. G. and J. A. Doolittle. 1985. Geophysical techniques for reconnaissance investigations of soils and surficial deposits in mountainous terrain. *Soil Science Society of America J.* 49: 1490-1498.

Puckett, W. E., M. E. Collins, and G. W. Schellentrager. 1990. Design of soil map units on a karst area in West Central Florida. *Soil Science Society of America J.* 54:1068-1073.

Schellentrager G. W. and J. A. Doolittle. 1985. Evaluating subsidence of Histosols in the Everglade Agricultural Area using ground-penetrating radar. Final Report. USDA-Soil Conservation Service, Gainesville, Florida. pp. 40.

Schellentrager, G. W., J. A. Doolittle, T. E. Calhoun, and C. A. Wettstein. 1988. Using ground-penetrating radar to update soil survey information. *Soil Science Society of America J.* 52:746-752.

Shih, S. F. and J. A. Doolittle. 1984. Using radar to investigate organic soil thickness in the Florida Everglades. *Soil Science Society of America J.* 48:651-656.

Shih, S. F., J. A. Doolittle, D. L. Myhre, and G. W. Schellentrager. 1986. Using radar for groundwater investigation. *J. Irrigation and Drainage Engineering.* 112(2):110-118.

Shih, S. F., D. L. Myhre, G. W. Schellentrager, V. W. Carlisle, and J. A. Doolittle. 1985a. Using radar to assess the soil characteristics related to citrus stress. *Soil and Crop Science of Florida, Proc.* 45:54-59.

Soil Survey Staff. 1992. Keys to Soil Taxonomy. USDA-Soil Management Support Service Technical Monograph No. 19. Pocahontas Press, Inc. Blacksburg, VA. pp. 541.

Electromagnetic Induction Methods

Electromagnetic inductive (EM) is a surface-geophysical method in which electromagnetic energy is used to measure the terrain or apparent conductivity of earthen materials. This technique has been used extensively to monitor groundwater quality and potential seepage from waste sites (Brune and Doolittle, 1990; Byrnes and Stoner, 1988; De Rose, 1986; Greenhouse and Slaine, 1983; Greenhouse et al., 1987; and Siegrist and Hargett, 1989)

For surveying, the meter is placed on the ground surface or held above the surface at a specified distance. A power source within the meter generates an alternating current in the transmitter coil. The current flow produces a primary magnetic field and induces electrical currents in the soil. The induced current flow is proportional to the electrical conductivity of the intervening medium. The electrical currents create a secondary magnetic field in the soil. The secondary magnetic field is of the same frequency as the primary field but of different phase and direction. The primary and secondary fields are measured as a change in the potential induced in the receiver coil. At low transmission frequency, the ratio of the secondary to the primary magnetic field is directly proportional to the ground conductivity. Values of apparent conductivity are expressed in milliSiemens per meter (mS/m).

Electromagnetic methods measure the apparent conductivity of earthen materials. Apparent conductivity is the weighted average conductivity measurement for a column of earthen materials to a specified penetration depth (Greenhouse and Slaine; 1983). The averages are weighted according to the depth response function of the meter (Slavich and Petterson, 1990).

Variations in the meters response are produced by changes in the ionic concentration of earthen materials which reflects changes in sediment type, degree of saturation, nature of the ions in solution, and metallic objects. Factors influencing the conductivity of earthen materials include: (i) the volumetric water content, (ii) the amount and type of ions in the soil water, (iii) the amount and type of clays in the soil matrix, and (iv) the soil temperature. Williams and Baker (1982), and Williams (1983) observed that, in areas of salt affected soils, 65 to 70 percent of the variation in measurements could be explained by the concentration of soluble salts. However, as water provides the electrolytic solution through which the current must pass, a threshold level of moisture is required in order to obtain meaningful results (Van der Lelij, 1983).

The depth of penetration is dependent upon the intercoil spacing, transmission frequency, and coil orientation relative to the ground surface. The anticipated depths of measurements for the EM38 meter is 0.75 m and 1.5 m in the horizontal and vertical dipole

orientations, respectively. The actual depth of measurement will depend on the conductivity of the earthen material(s) scanned.

The conductivity meters provide limited vertical resolution and depth information. However, as discussed by Benson and others (1984), the absolute EM values are not necessarily diagnostic in themselves, but lateral and vertical variations in these measurements are significant. The seasonal variation in soil conductivity (produced by variations in soil moisture and temperature) can be added to the statement by Benson. Interpretations of the EM data are based on the identification of spatial patterns in the data set appearing on two-dimensional contour plots.

References

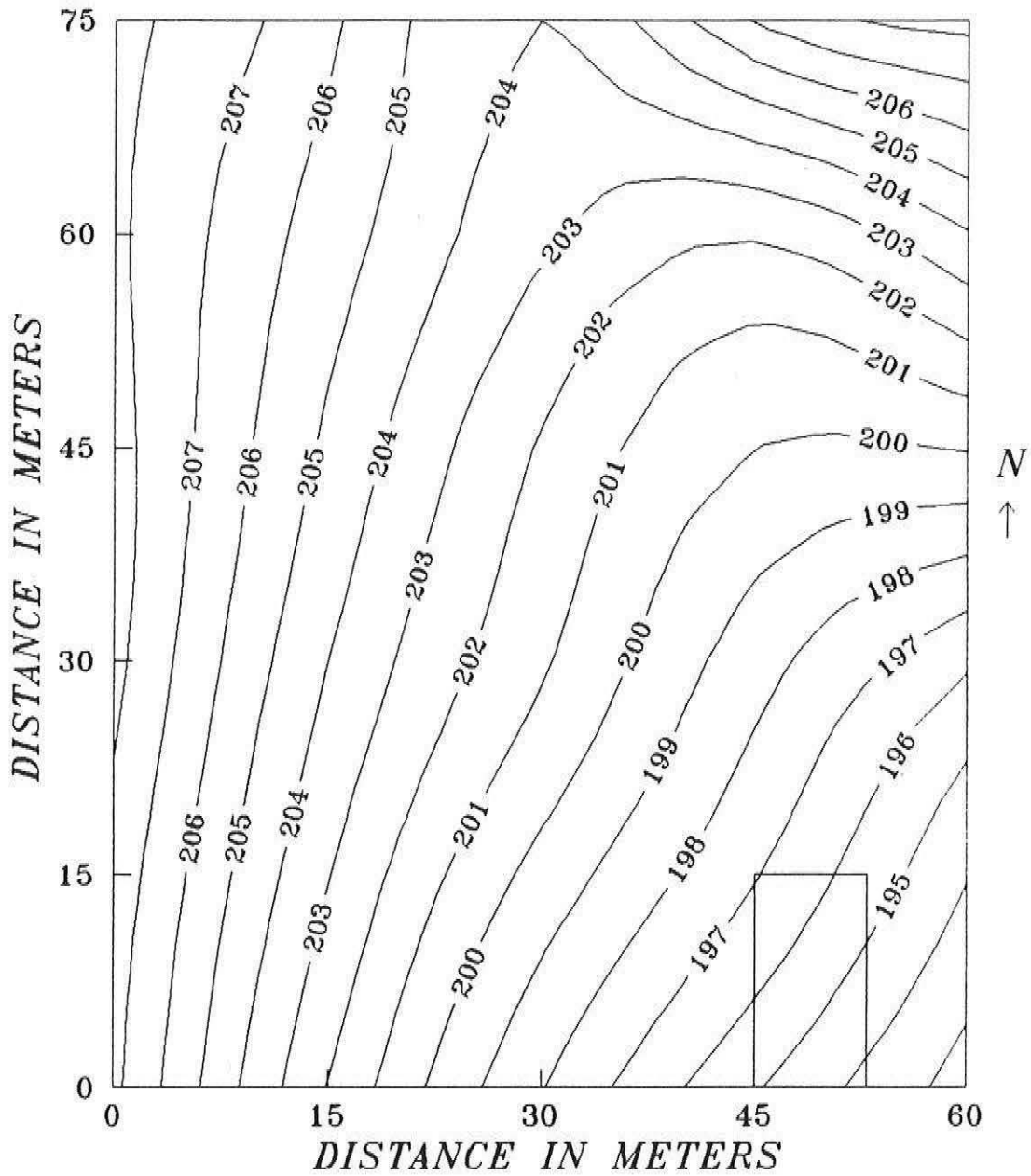
- Benson, R. C., R. A. Glaccum, and M. R. Noel. 1984. Geophysical techniques for sensing buried wastes and waste migration: an application review. IN: D. M. Nielsen and M. Curls (eds.) Surface and Borehole Geophysical Methods in Ground Water Investigations. NWWA/EPA Conference, San Antonio, Texas. p. 533-566.
- Brune, D. E. and J. Doolittle. 1990. Locating lagoon seepage with radar and electromagnetic survey. *Environ. Geol. Water Science* 16(3):195-207.
- Byrnes, T. R. and D. W. Stoner. 1988. Groundwater monitoring in karstic terrain; A case study of a landfill in northern New York. IN Proceeding of the FOCUS Conference on Eastern Regional Ground Water Issues. September 27-29 1988. Stamford, Connecticut. National Water Wells Assoc. Dublin, Ohio p. 53-76.
- De Rose, N. 1986. Applications of surface geophysical methods to ground water pollution investigations. IN: Evaluation of Pesticides in Ground Water. American Chemical Society, Washington, D.C. p. 118-140.
- Greenhouse, J. P., and D. D. Slaine. 1983. The use of reconnaissance electromagnetic methods to map contaminant migration. *Ground Water Monitoring Review* 3(2):47-59.
- Greenhouse, J. P., M. E. Monier-Williams, N. Ellert, and D. D. Slaine. 1987. Geophysical methods in groundwater contamination studies. In *Exploration '87 Proceedings. Application of Geophysics and Geochemistry*. p. 666-677.
- Siegrist, R. L. and D. L. Hargett. 1989. Application of surface geophysics for location of buried hazardous wastes. *Waste Management & Research* 7:325-335.
- Slavich, P. G. and G. H. Petterson. 1990. Estimating average rootzone salinity from electromagnetic induction (EM-38) measurements. *Aust. J. Soil Res.* 28:453-463.

Van der Lelij. A. 1983. Use of electromagnetic induction instrument (Type EM-38) for mapping soil salinity. Water Resource Commission, Murrumbidgee Div., N.S.W. Australia. pp. 14.

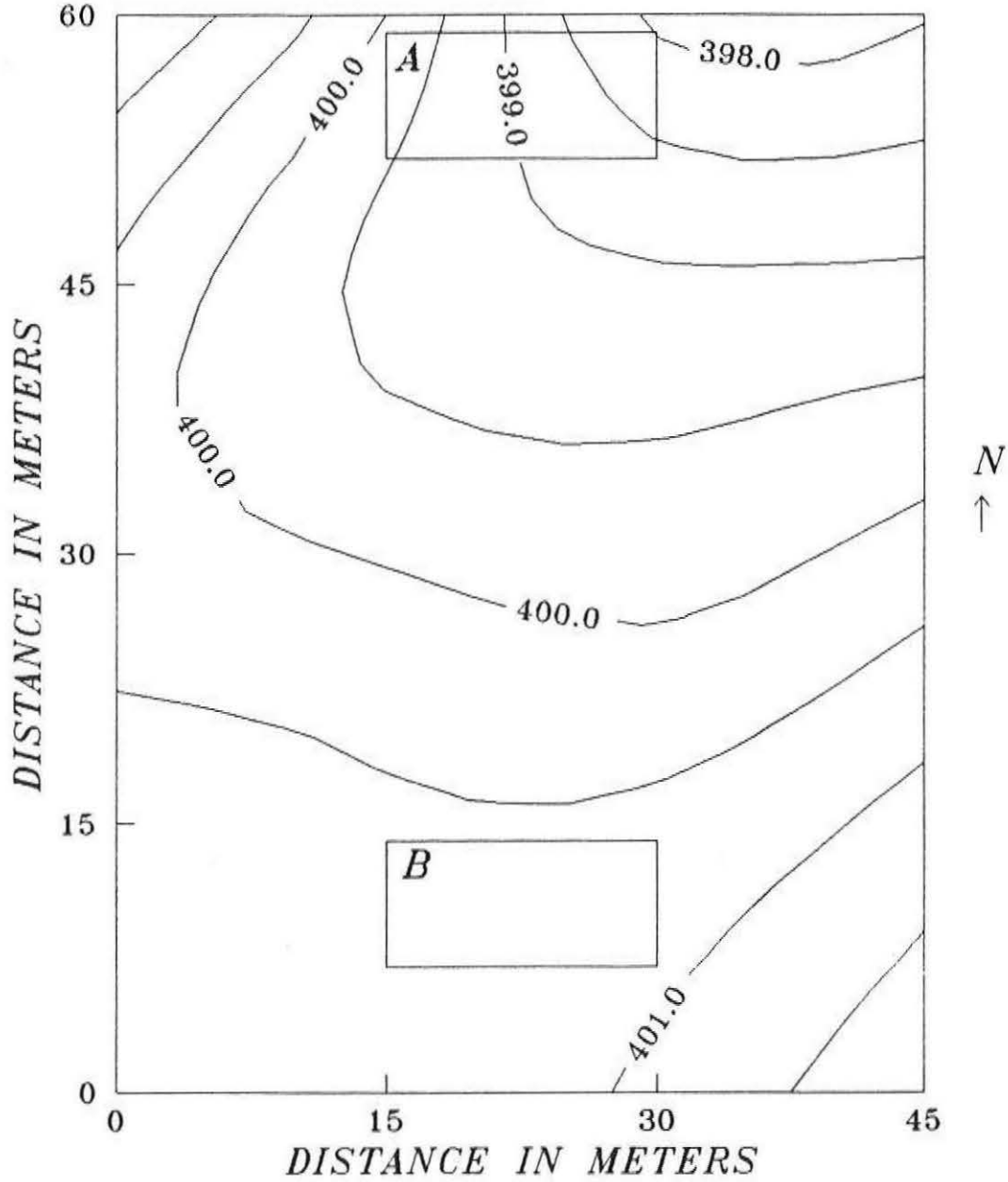
Williams, B. G. 1983. Electromagnetic induction as an aid to salinity investigations in northeast Thailand. CSIRO Inst. Biological Resources, Div. Water and Land Res. Canberra, Australia. Tech. Memo 83/27. pp. 7.

Williams, B. G. and G. C. Baker. 1982. An electromagnetic induction technique for reconnaissance surveys of soil salinity hazards. Australian J. Soil Res. 20(2):107-118.

TOPOGRAPHY OF BATTERSEA SITE
CONTOUR INTERVAL = 1 METER



TOPOGRAPHY OF MARTIN HILL SITE
CONTOUR INTERVAL = 0.5 METER



TOPOGRAPHY OF TRINITY SITE
CONTOUR INTERVAL = 0.5 METER

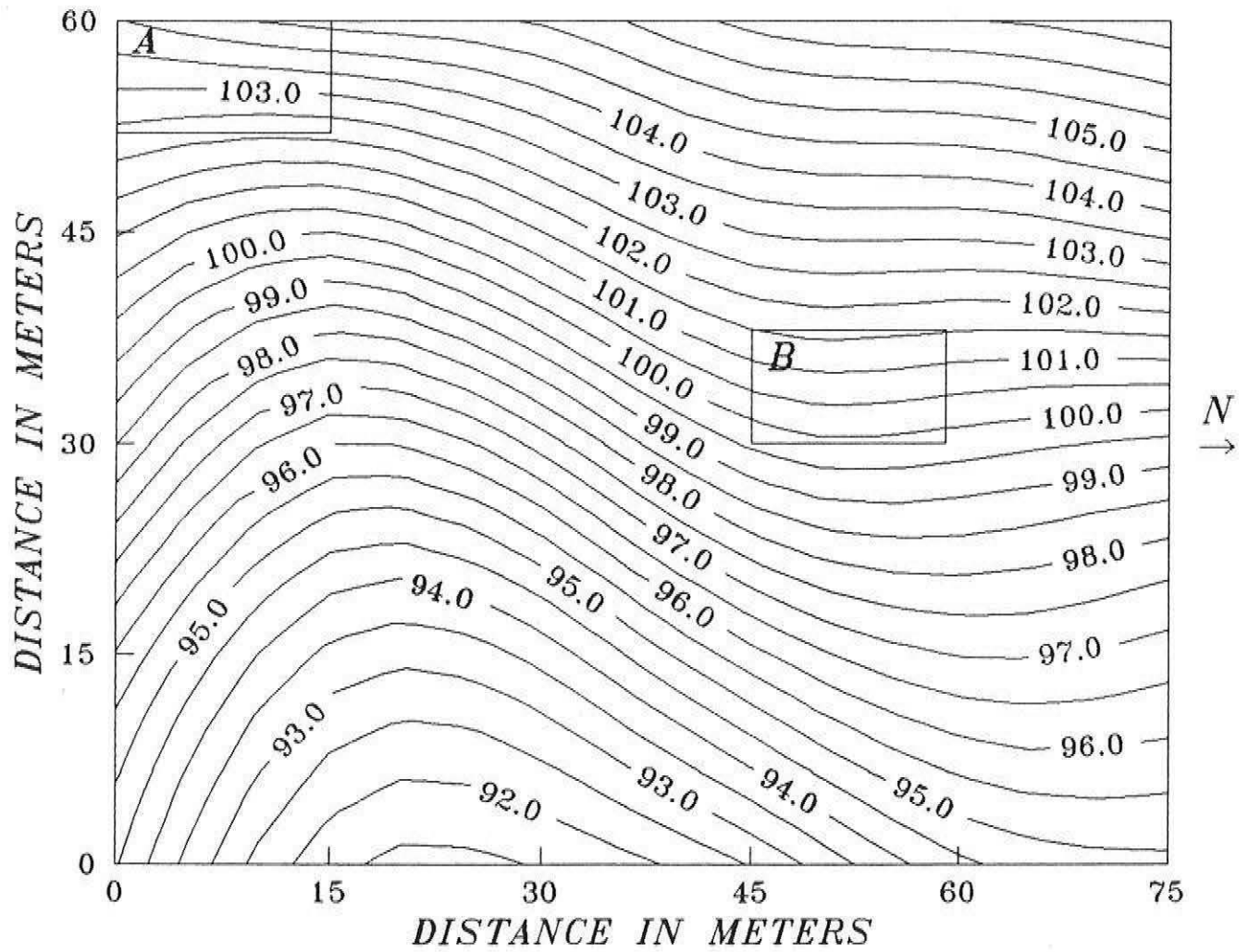


Figure 5

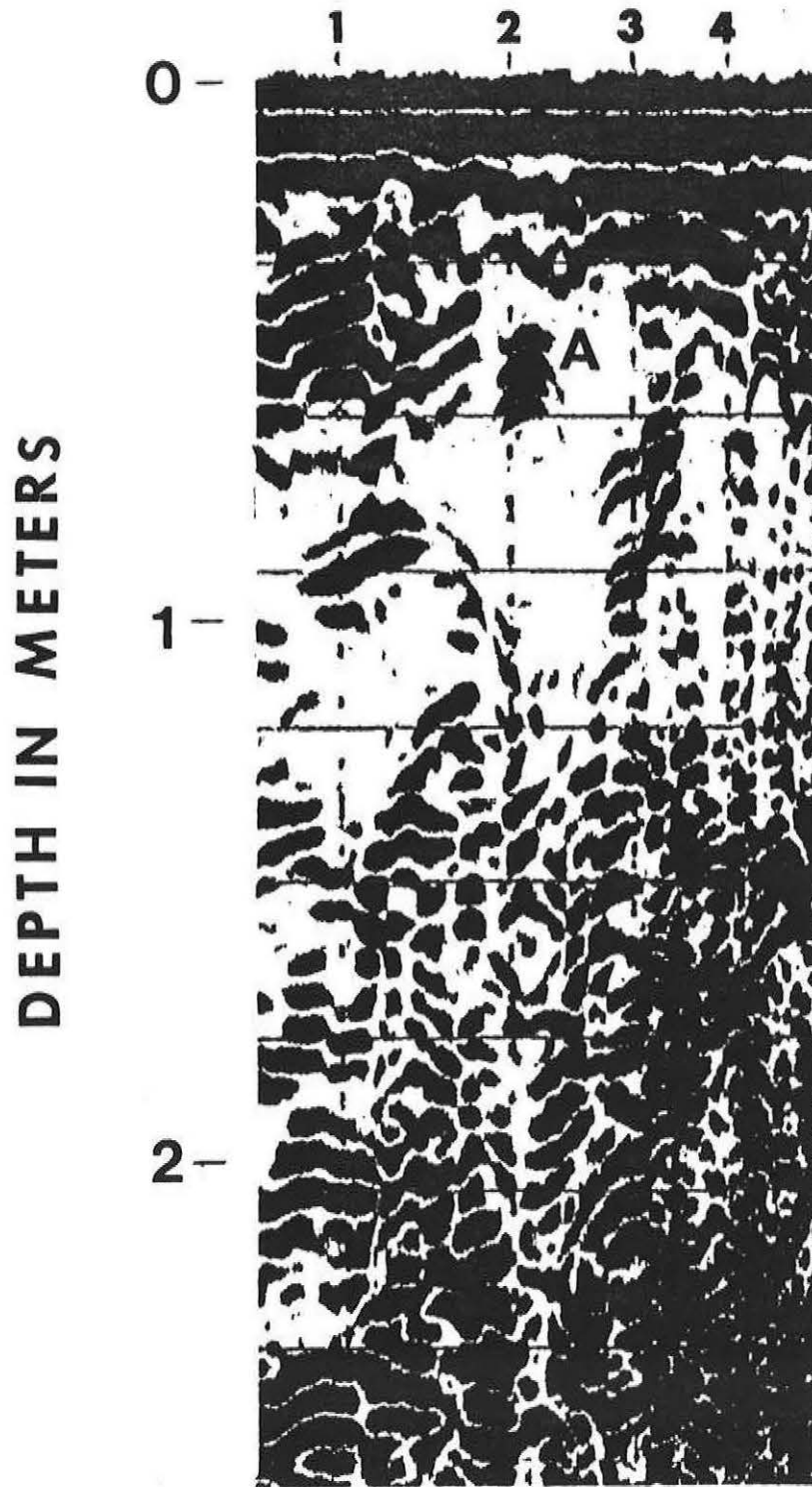
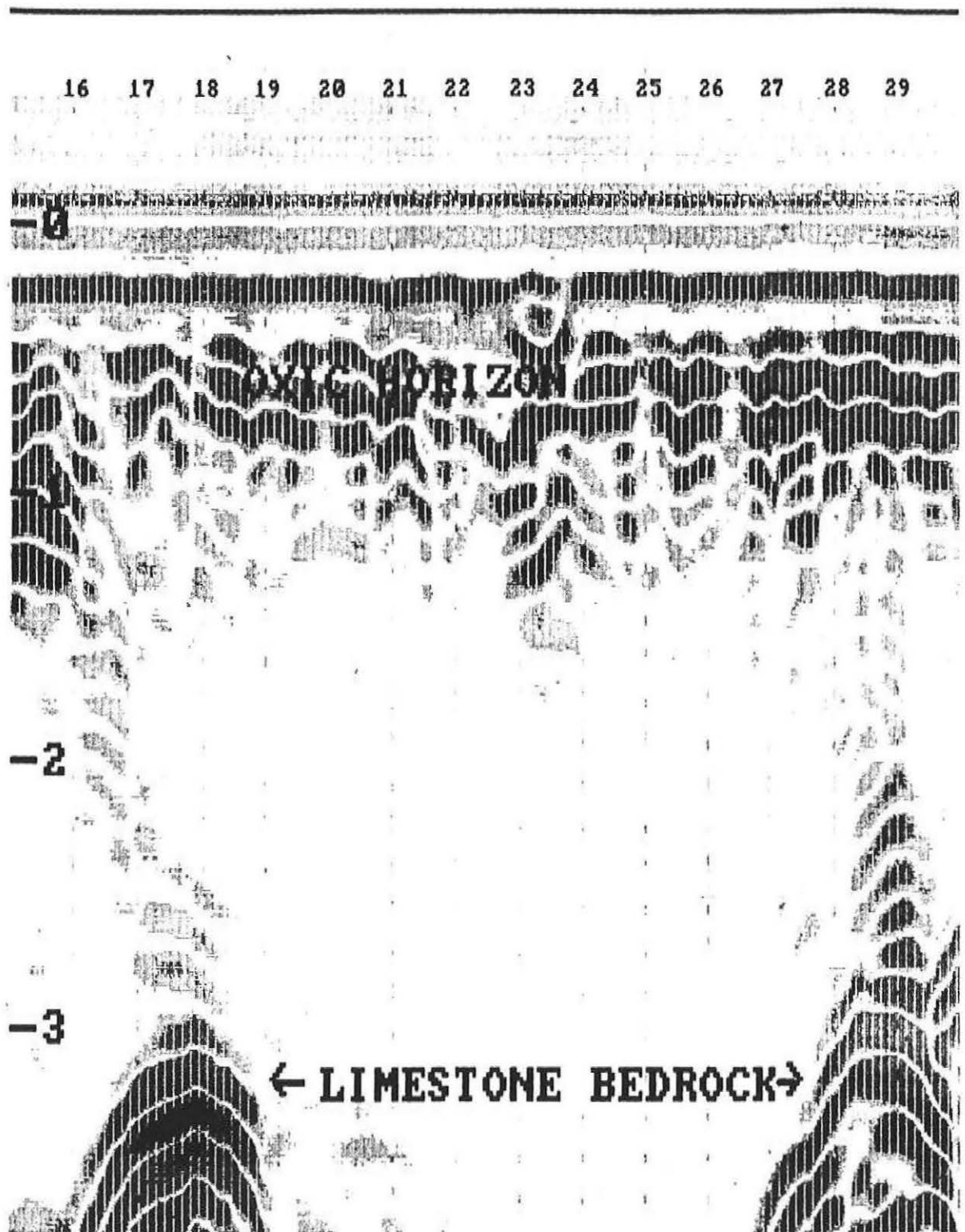
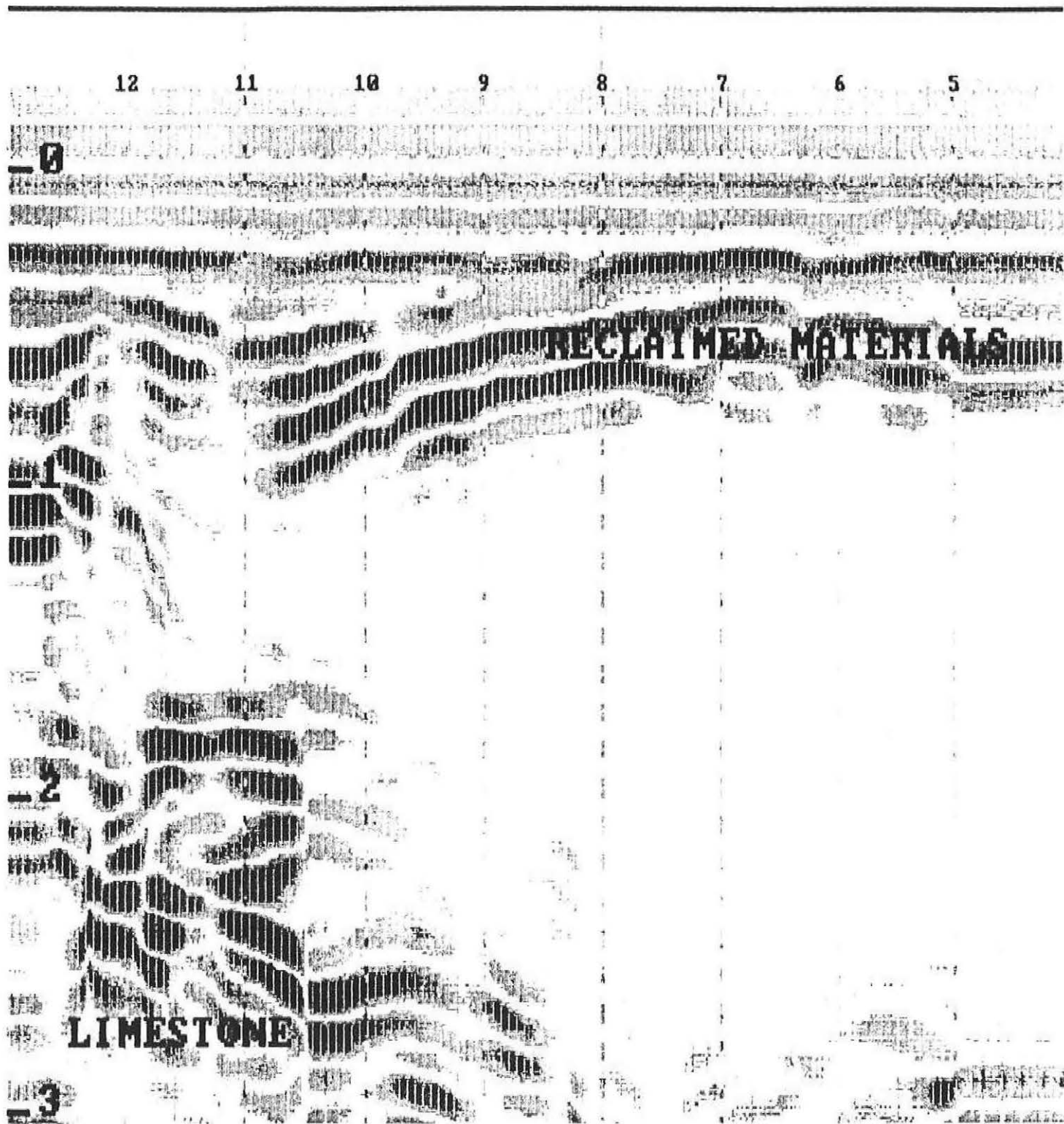
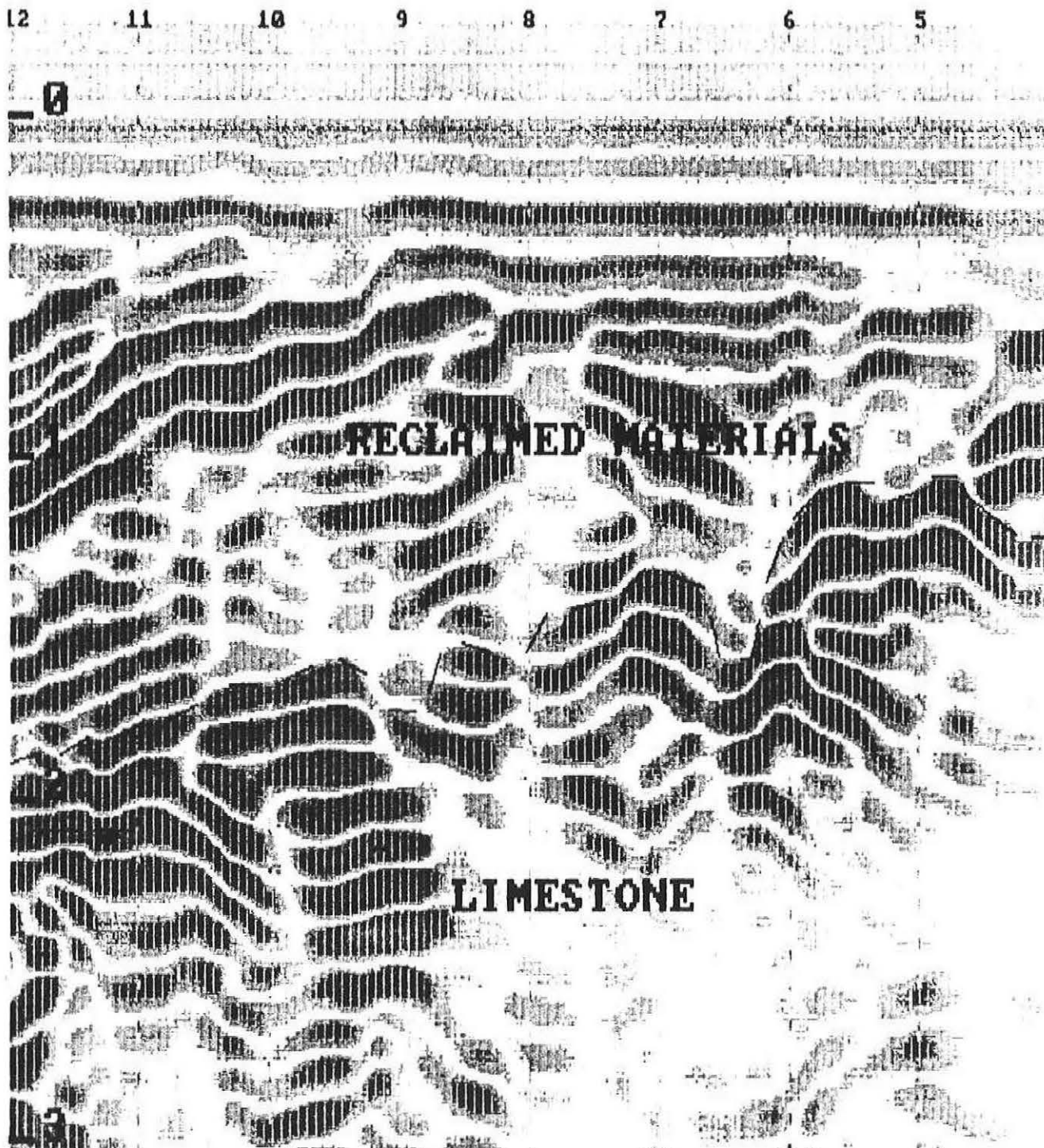


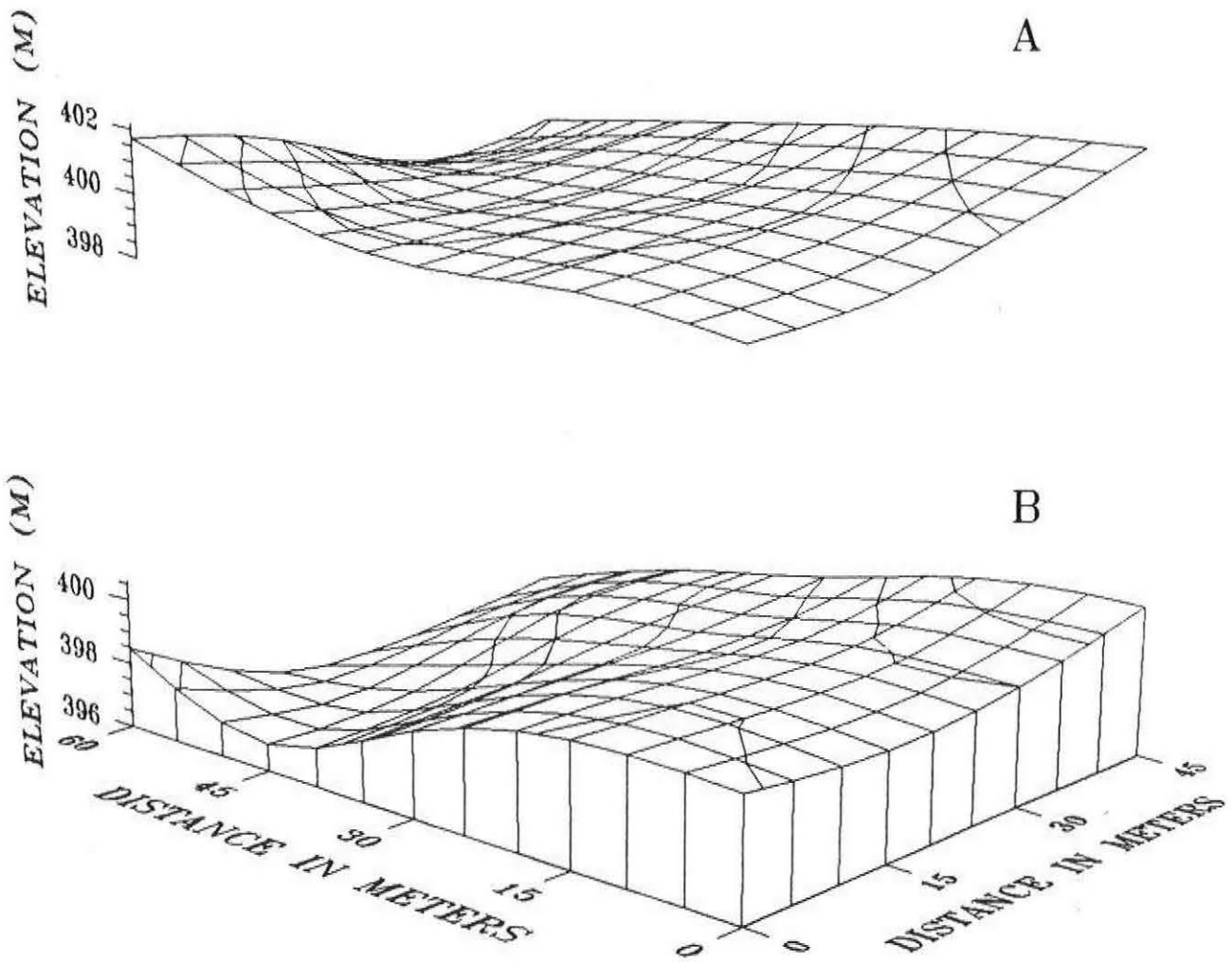
Figure 6







MARTIN HILL SITE - RELATIVE TOPOGRAPHY OF THE SOIL (A) AND BEDROCK (B) SURFACES.



MARTIN HILL SITE
DEPTH TO BEDROCK
CONTOUR INTERVAL = 0.25 METER

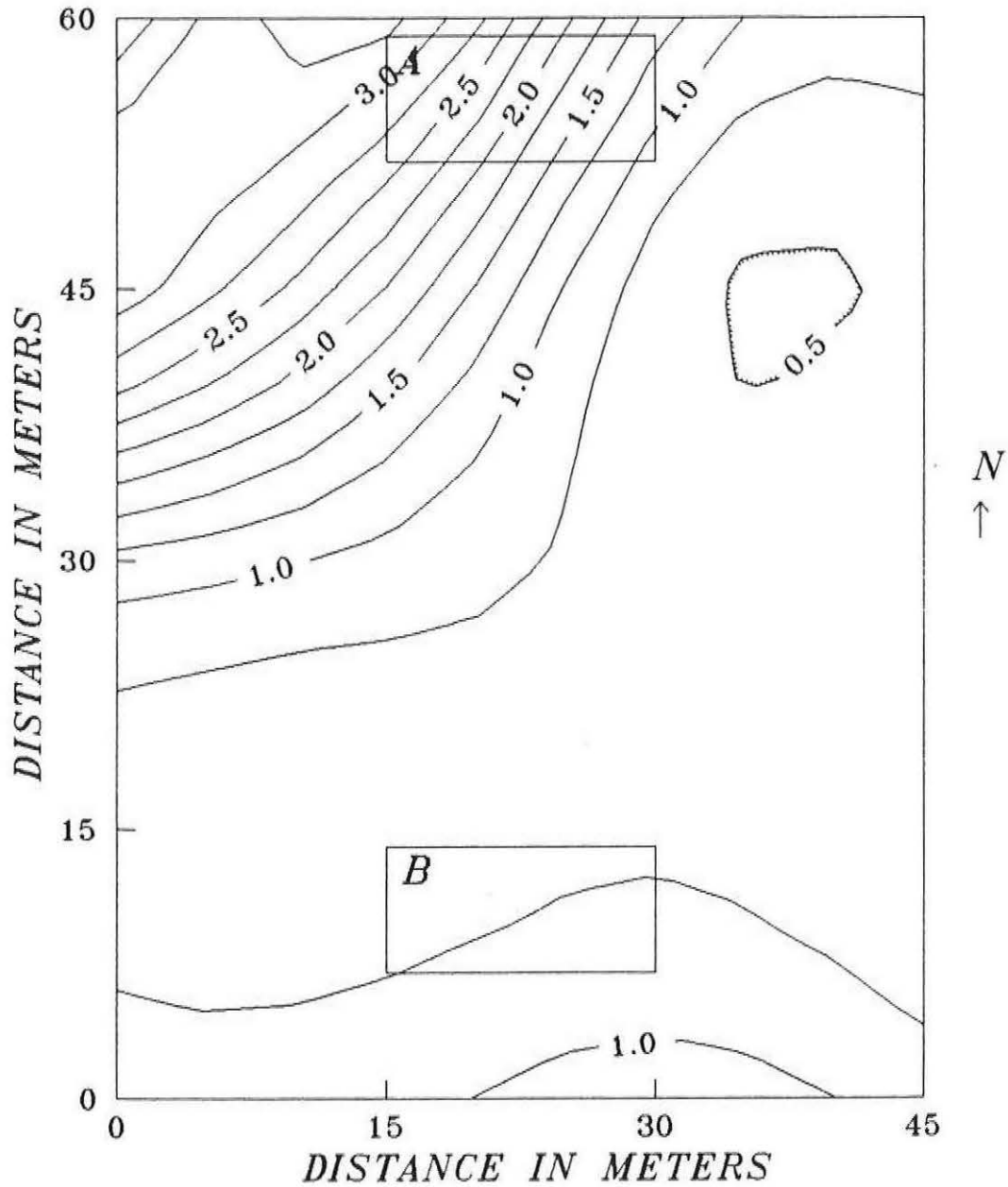
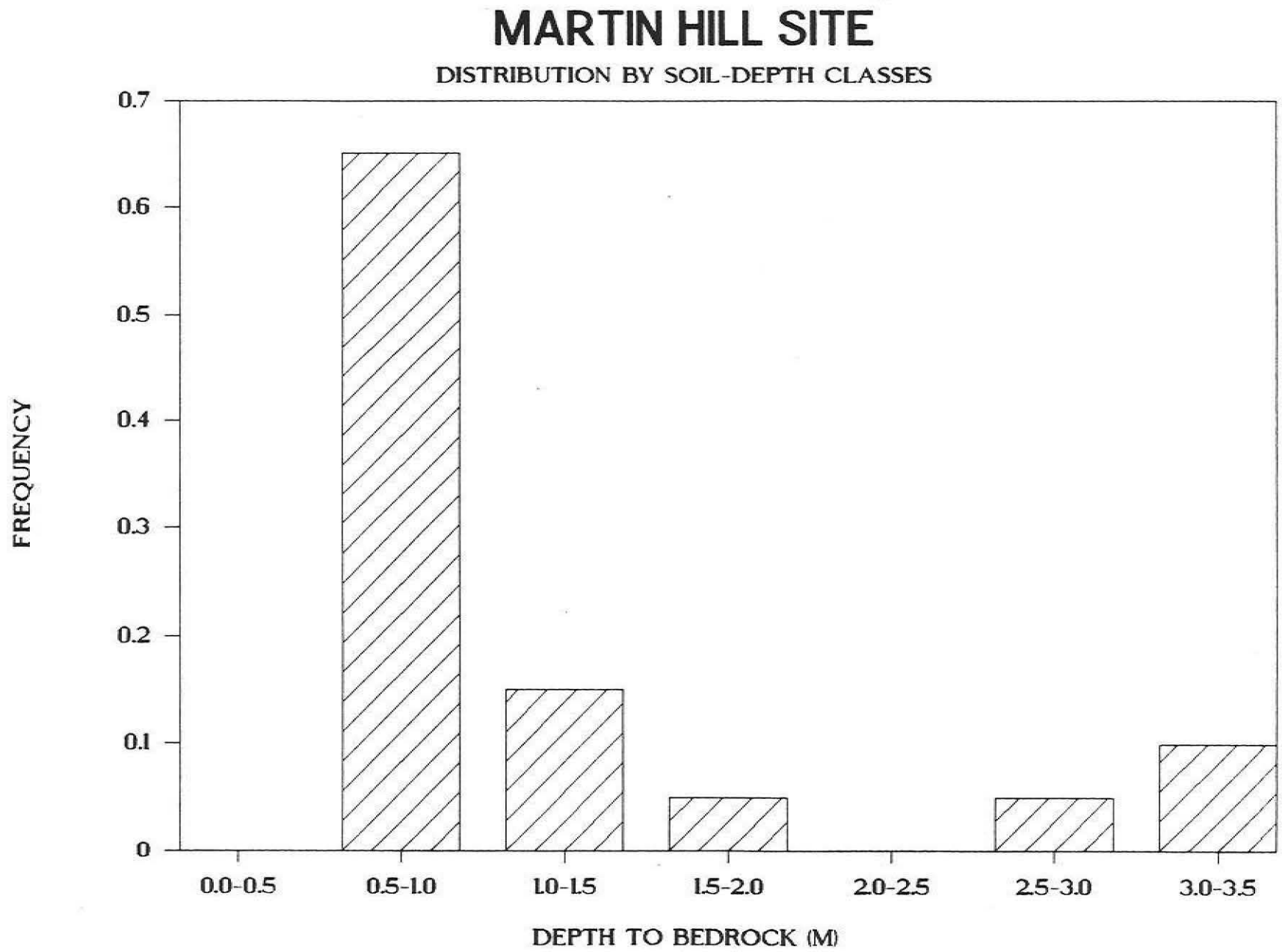
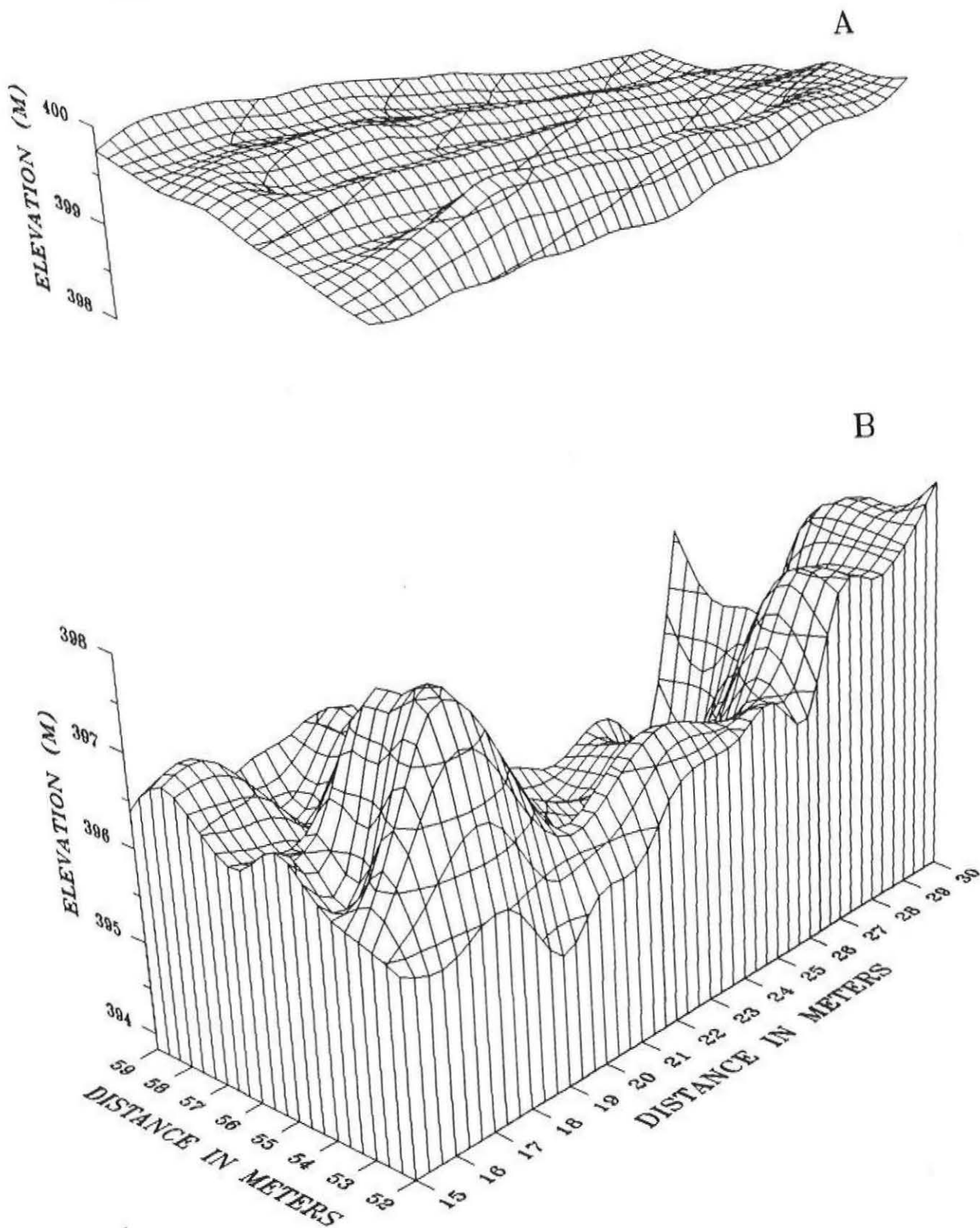


Figure 11



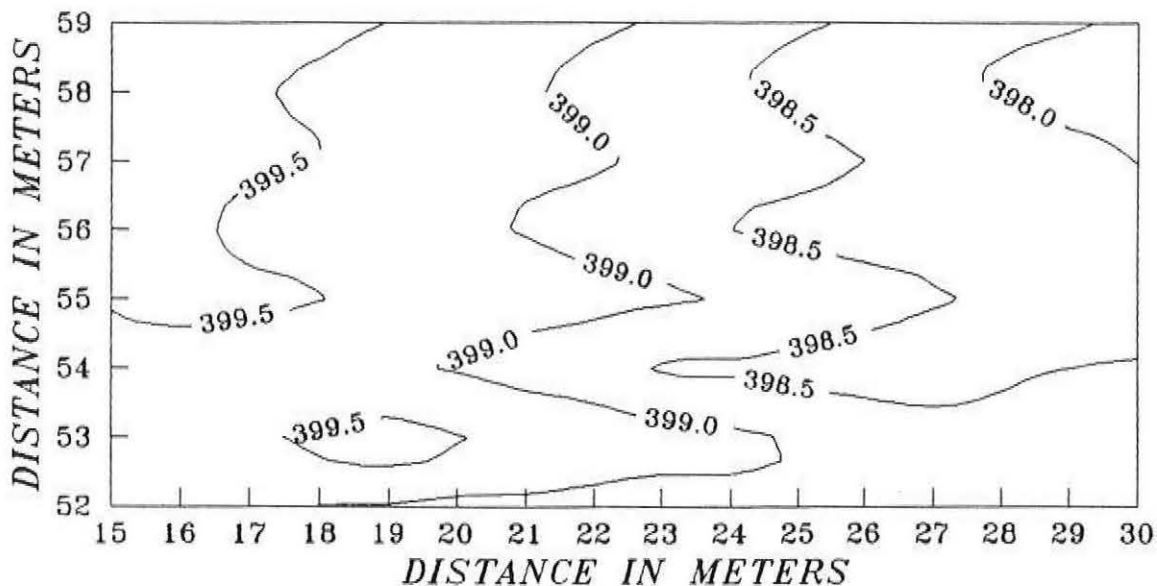
SUBSITE 'A' AT MARTIN HILL - RELATIVE TOPOGRAPHY
OF THE SOIL (A) AND BEDROCK (B) SURFACES.



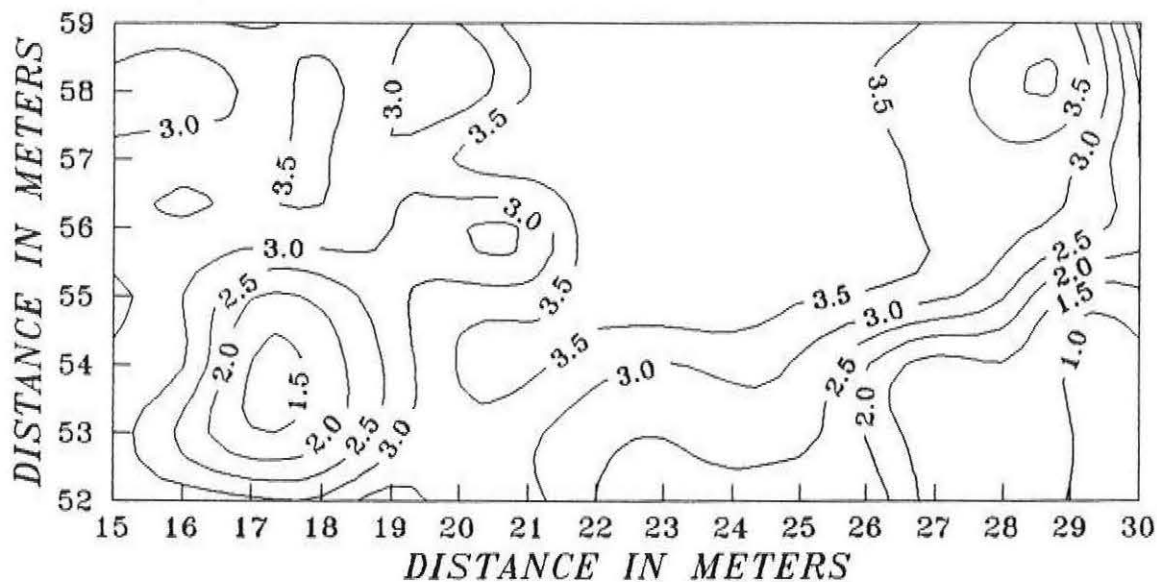
SUBSITE 'A' AT MARTIN HILL SITE
 RELATIVE TOPOGRAPHY OF SOIL SURFACE (A) AND
 DEPTH TO BEDROCK (B)

CONTOUR INTERVAL = 0.5 M

A

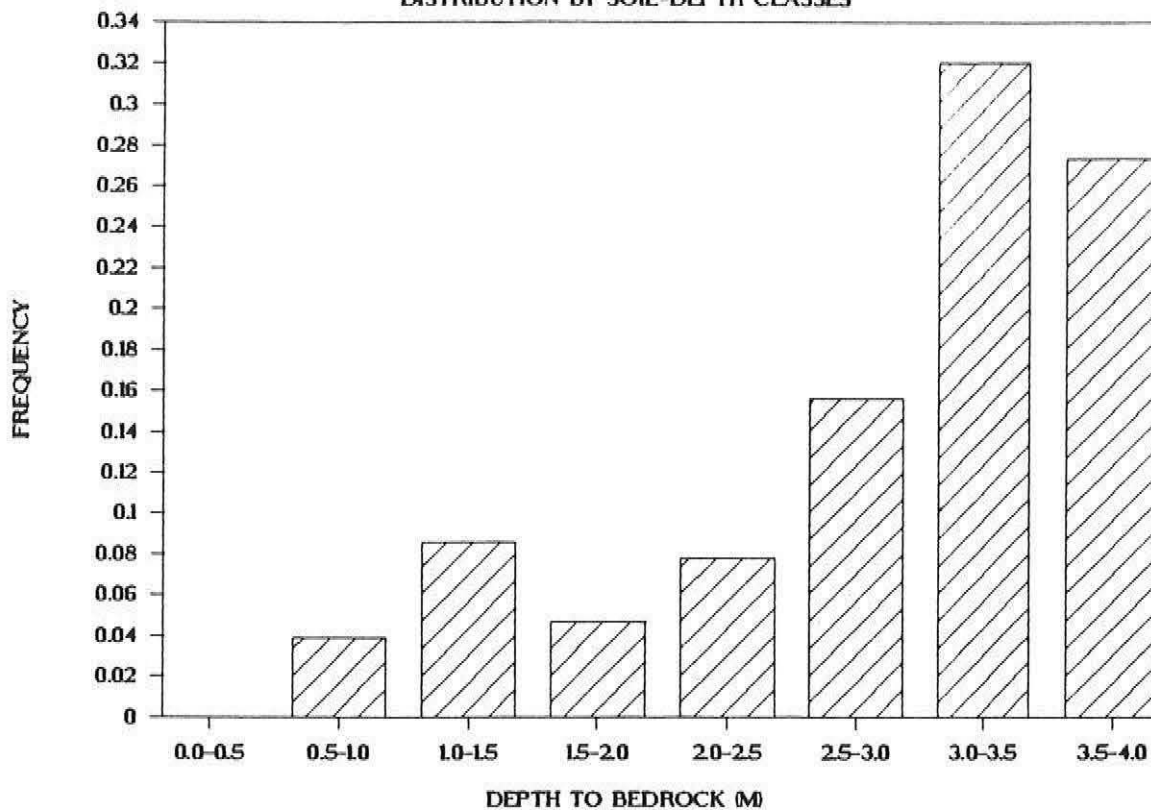


B



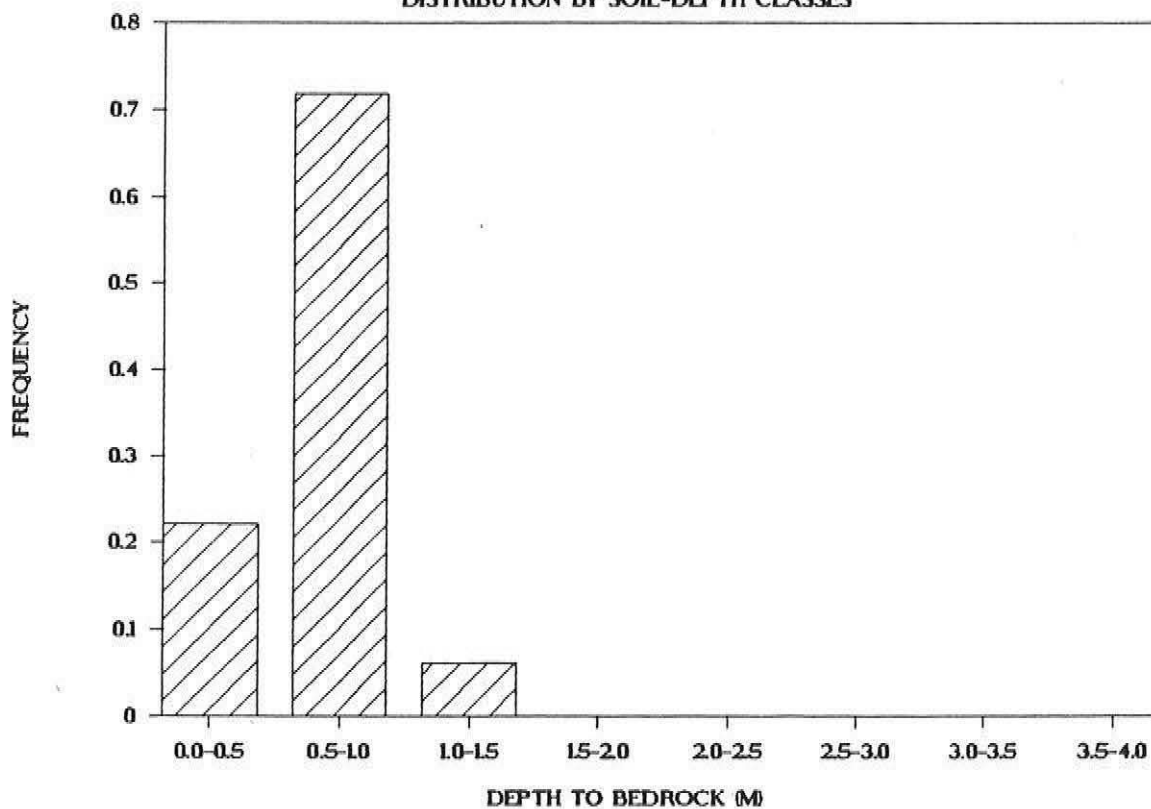
SUBSITE A - MARTIN HILL SITE

DISTRIBUTION BY SOIL-DEPTH CLASSES



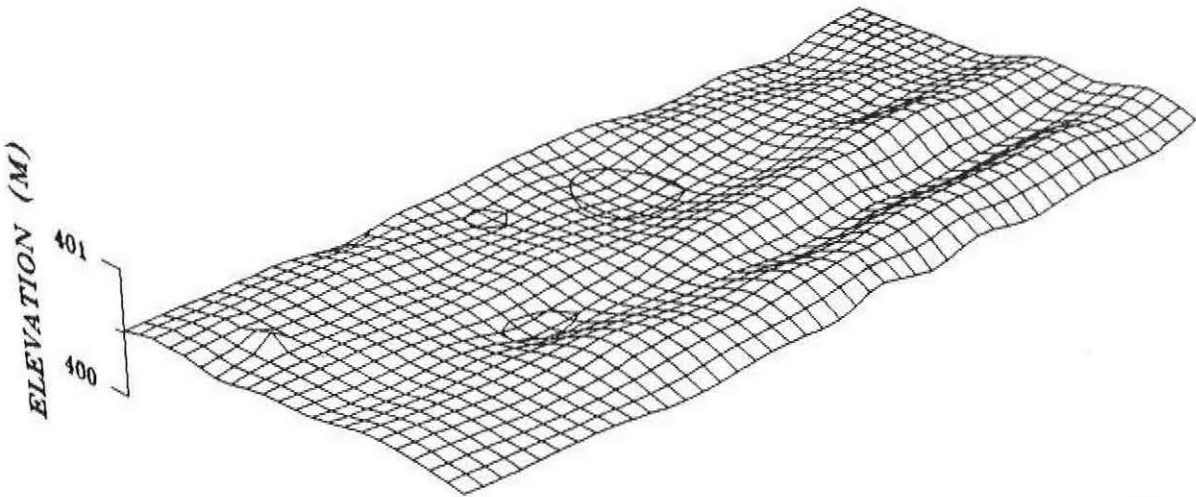
SUBSITE B - MARTIN HILL SITE

DISTRIBUTION BY SOIL-DEPTH CLASSES

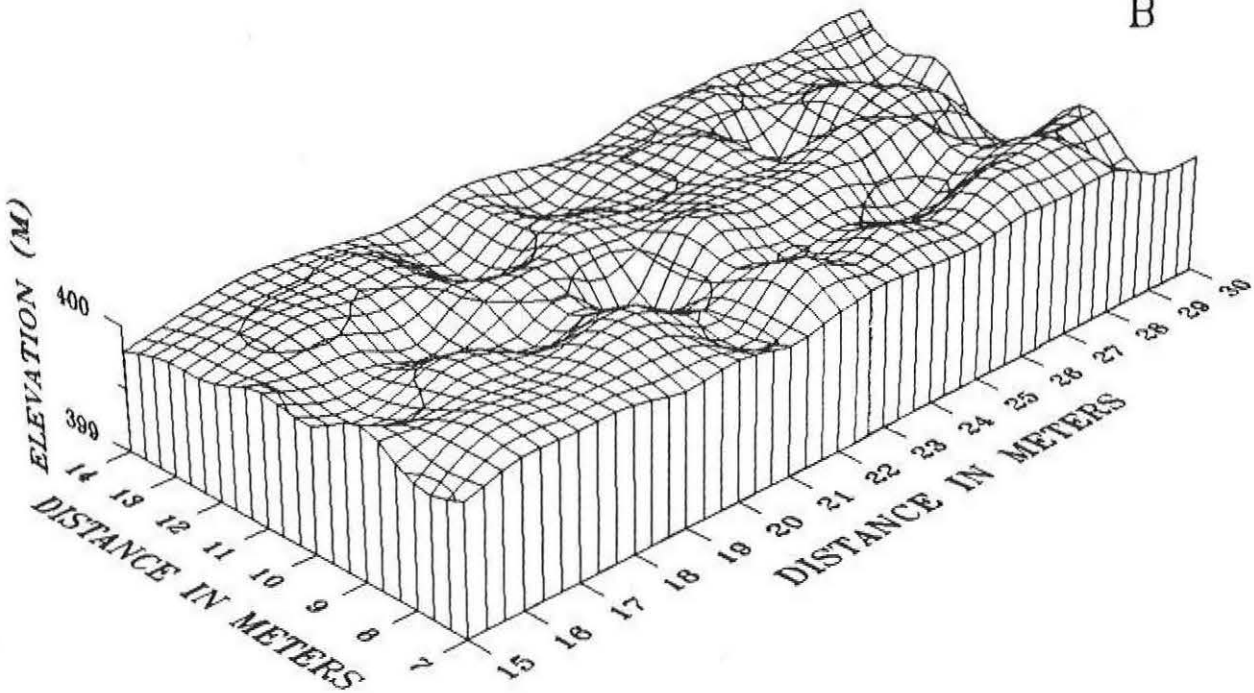


SUBSITE 'B' AT MARTIN HILL - RELATIVE TOPOGRAPHY OF THE SOIL (A) AND BEDROCK (B) SURFACES.

A



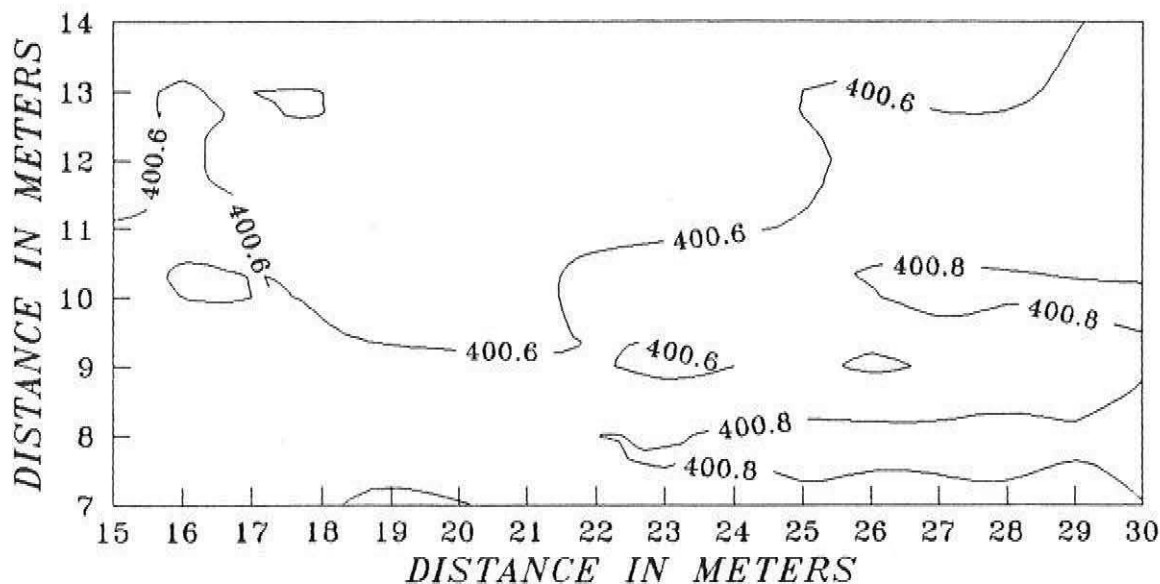
B



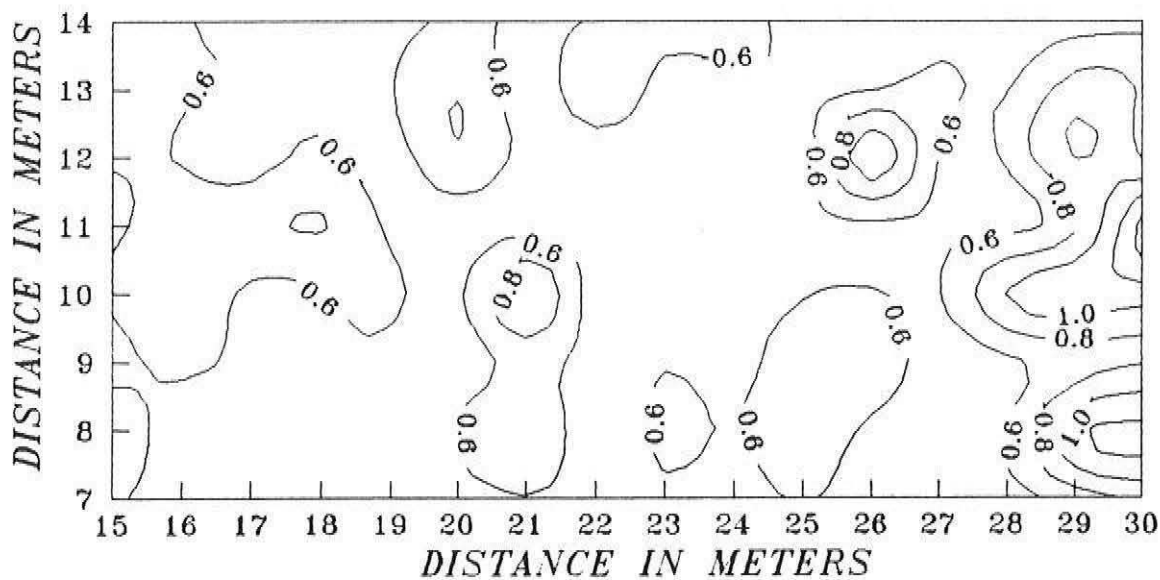
SUBSITE 'B' AT MARTIN HILL SITE
 RELATIVE TOPOGRAPHY OF SOIL SURFACE (A) AND
 DEPTH TO BEDROCK (B)

CONTOUR INTERVAL = 0.2 M

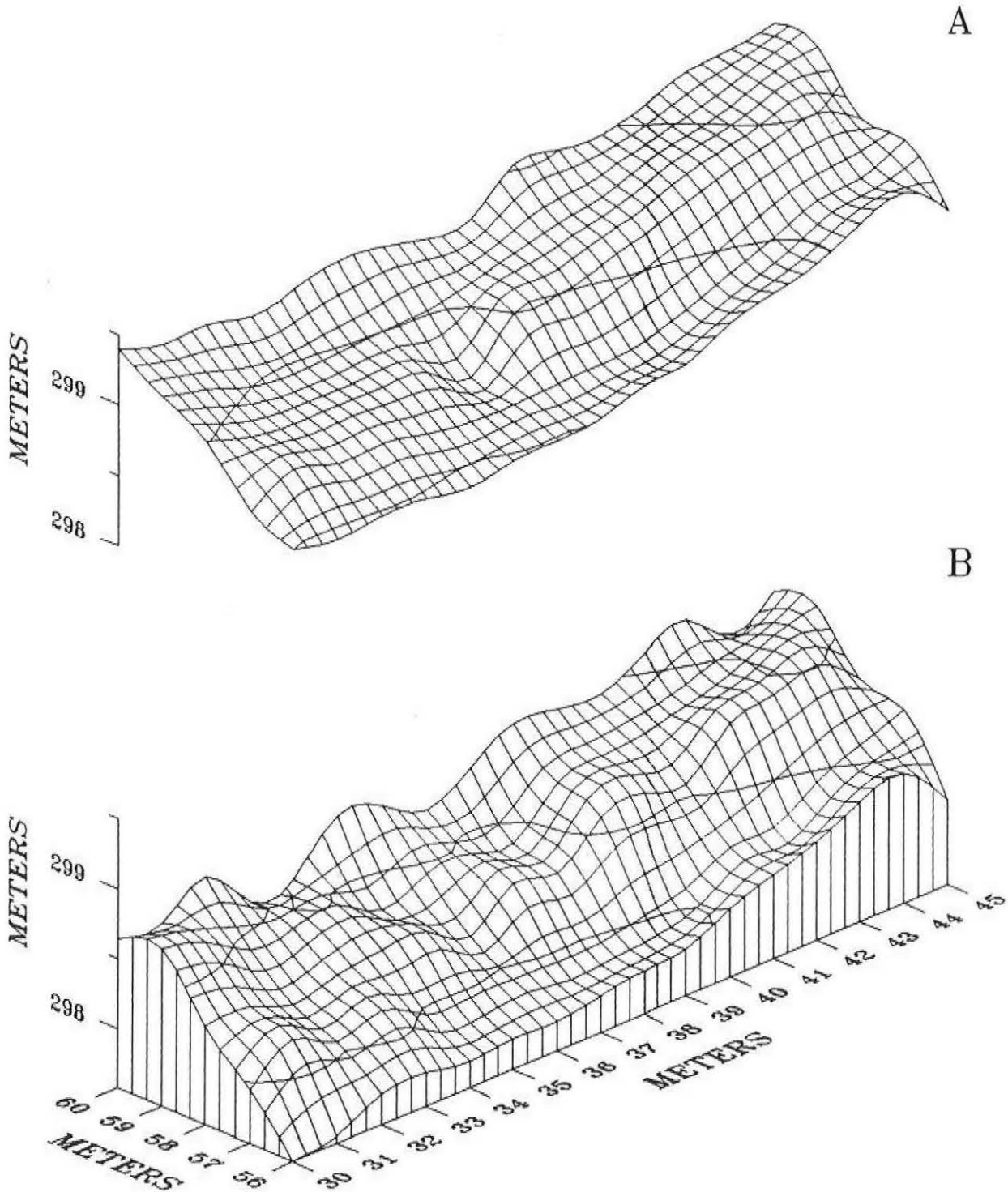
A



B



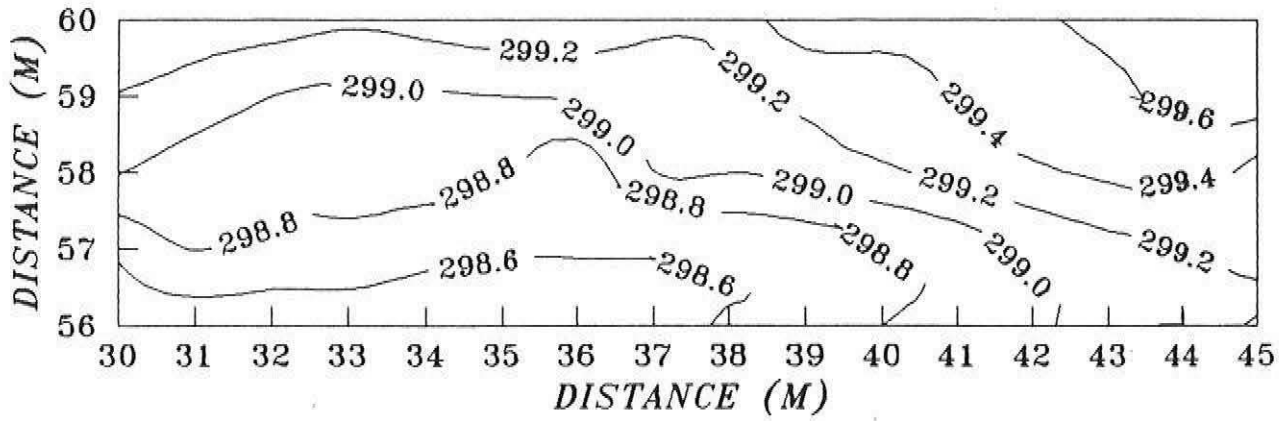
SUBSITE 'A' AT RUSSELL PLACE - RELATIVE TOPOGRAPHY OF THE SOIL (A) AND BEDROCK (B) SURFACES.



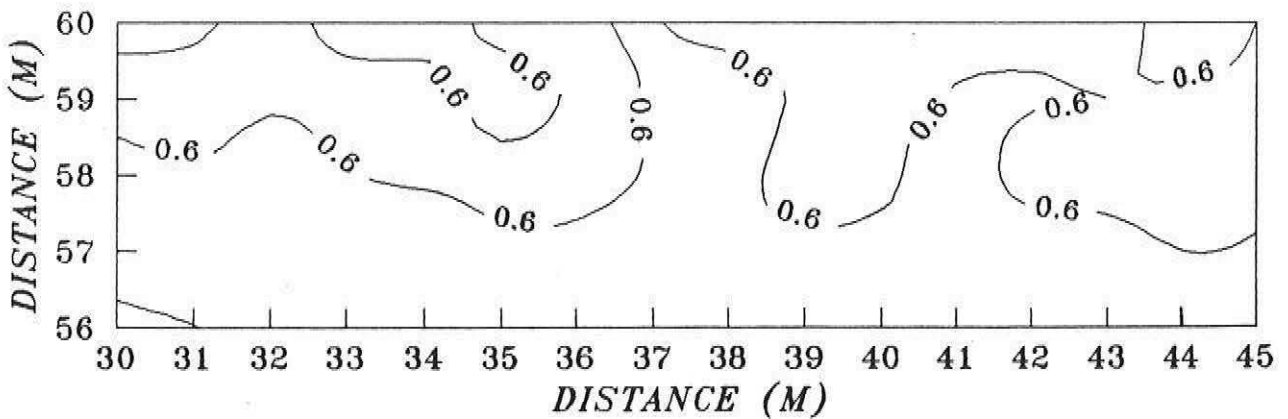
SUBSITE 'A' AT RUSSELL PLACE
RELATIVE TOPOGRAPHY OF SOIL SURFACE (A)
AND DEPTH TO BEDROCK (B)

CONTOUR INTERVAL = 0.2 M

A

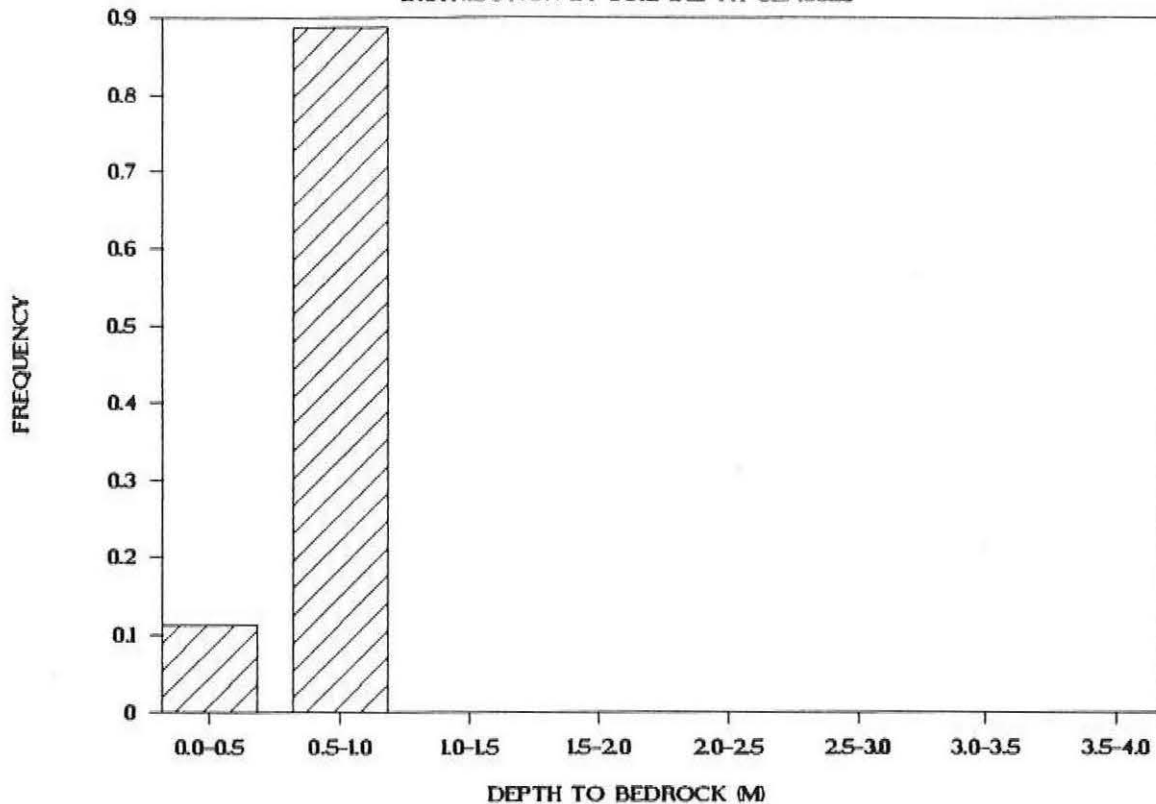


B



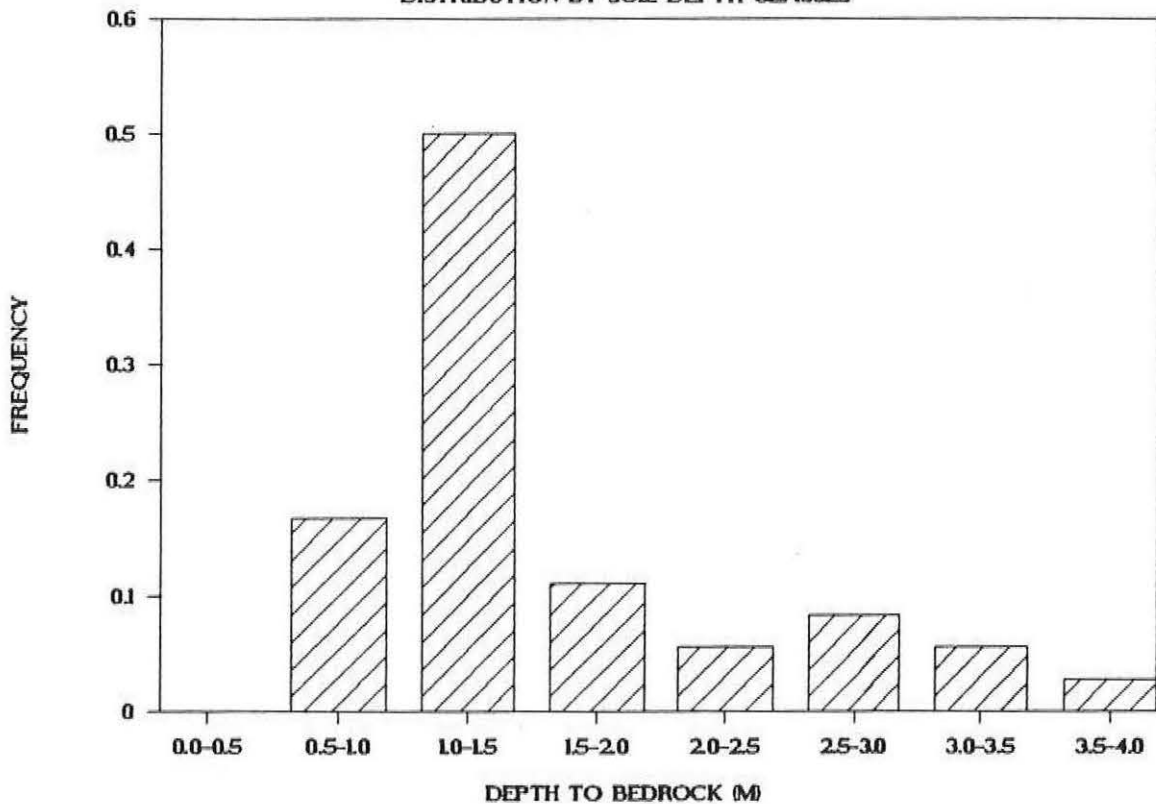
SUBSITE A - RUSSELL PLACE SITE

DISTRIBUTION BY SOIL DEPTH CLASSES

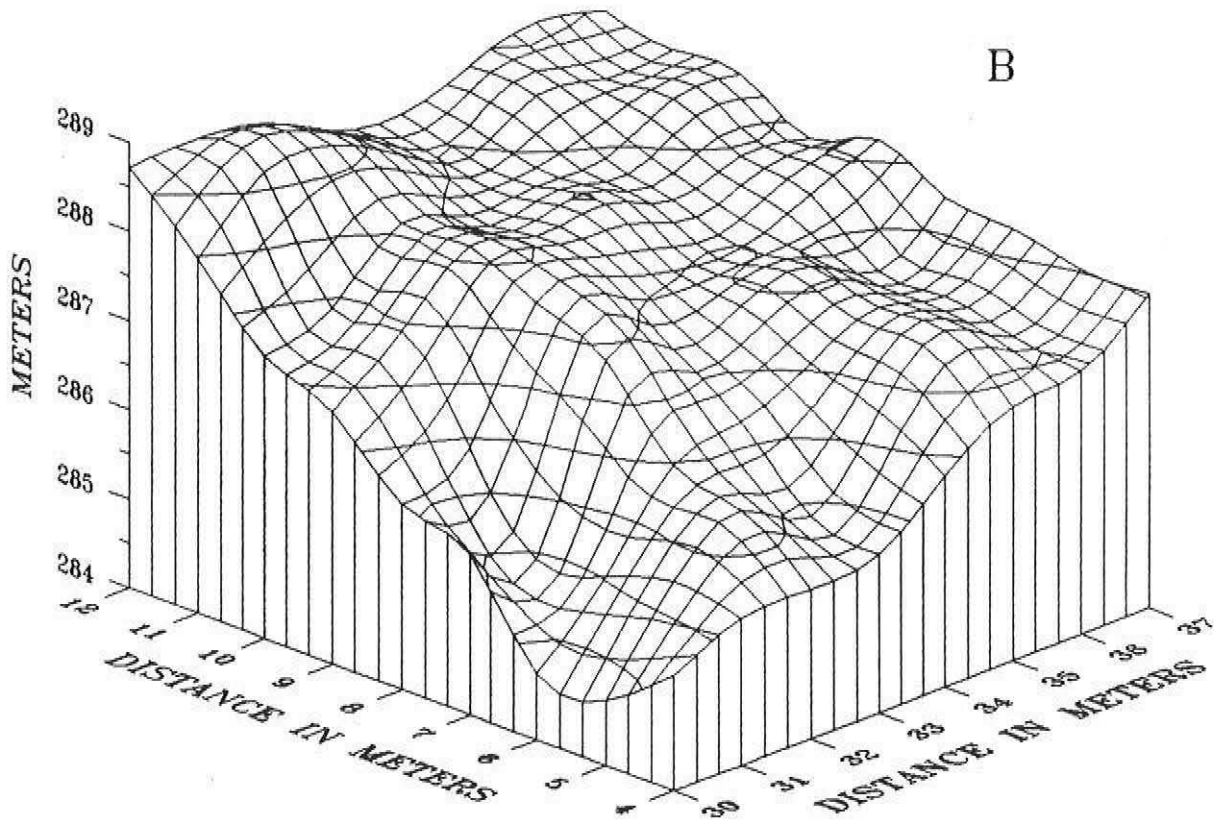
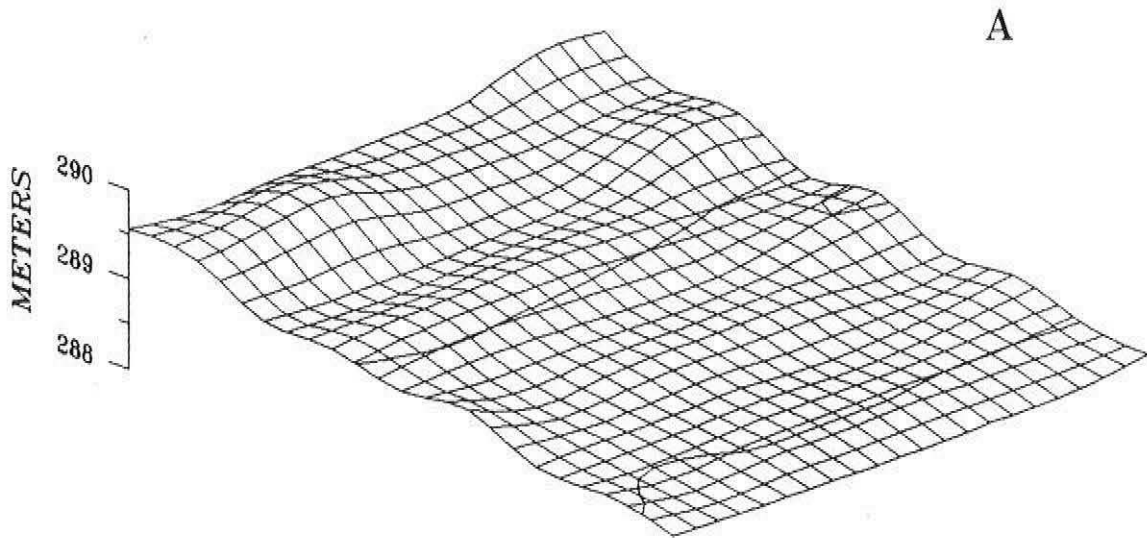


SUBSITE B - RUSSELL PLACE SITE

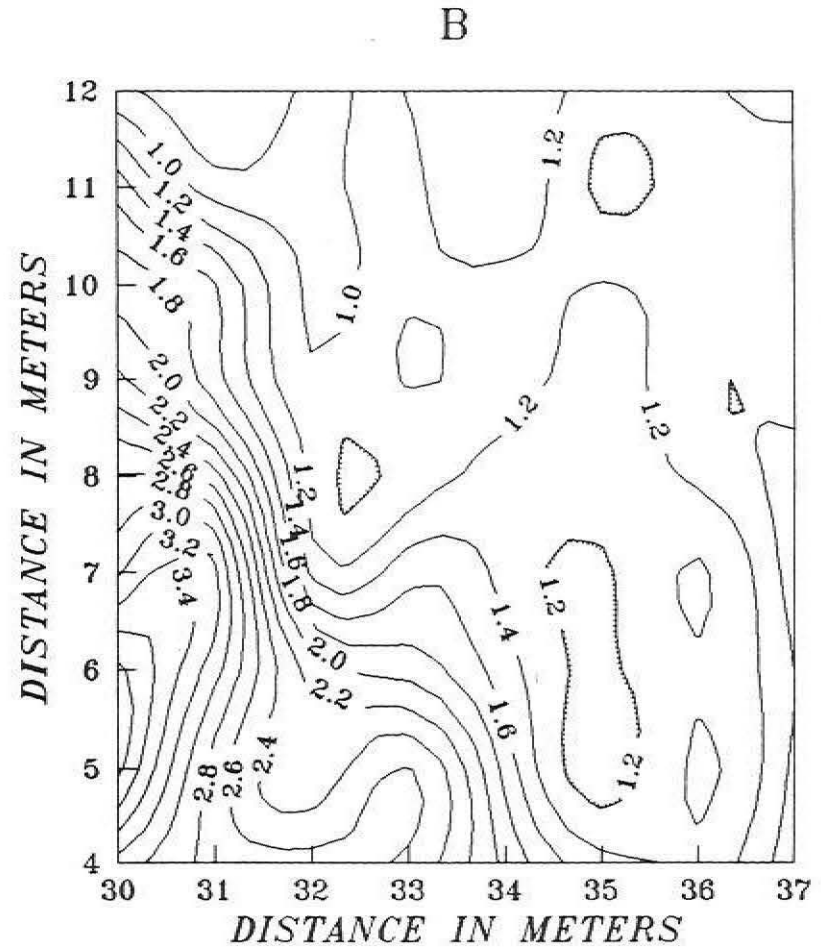
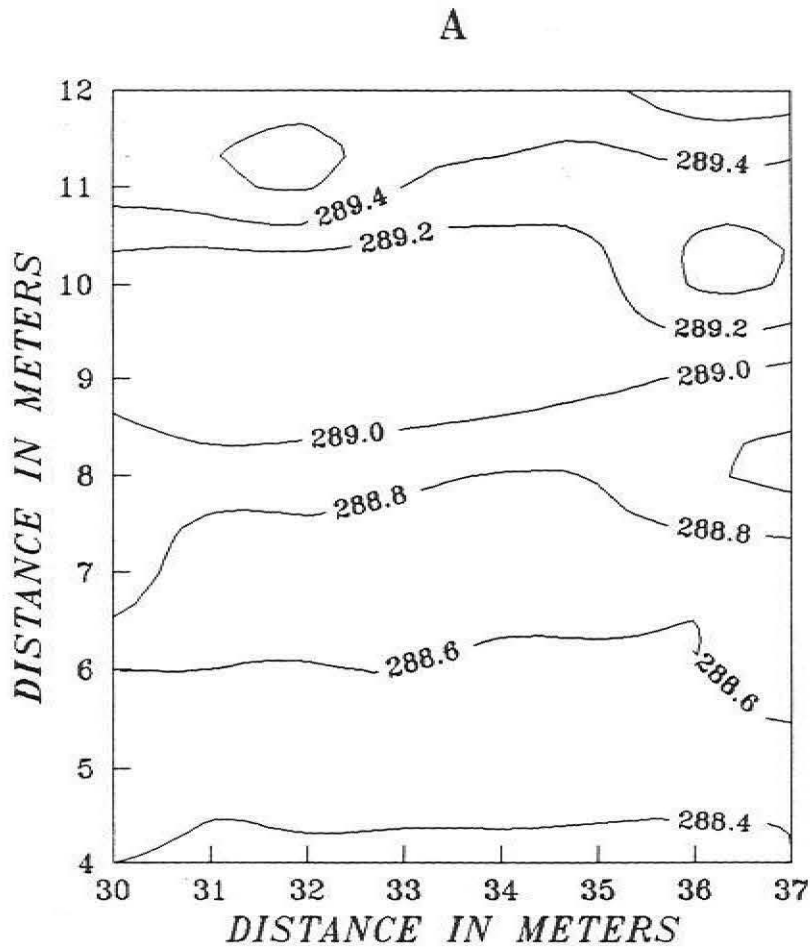
DISTRIBUTION BY SOIL DEPTH CLASSES



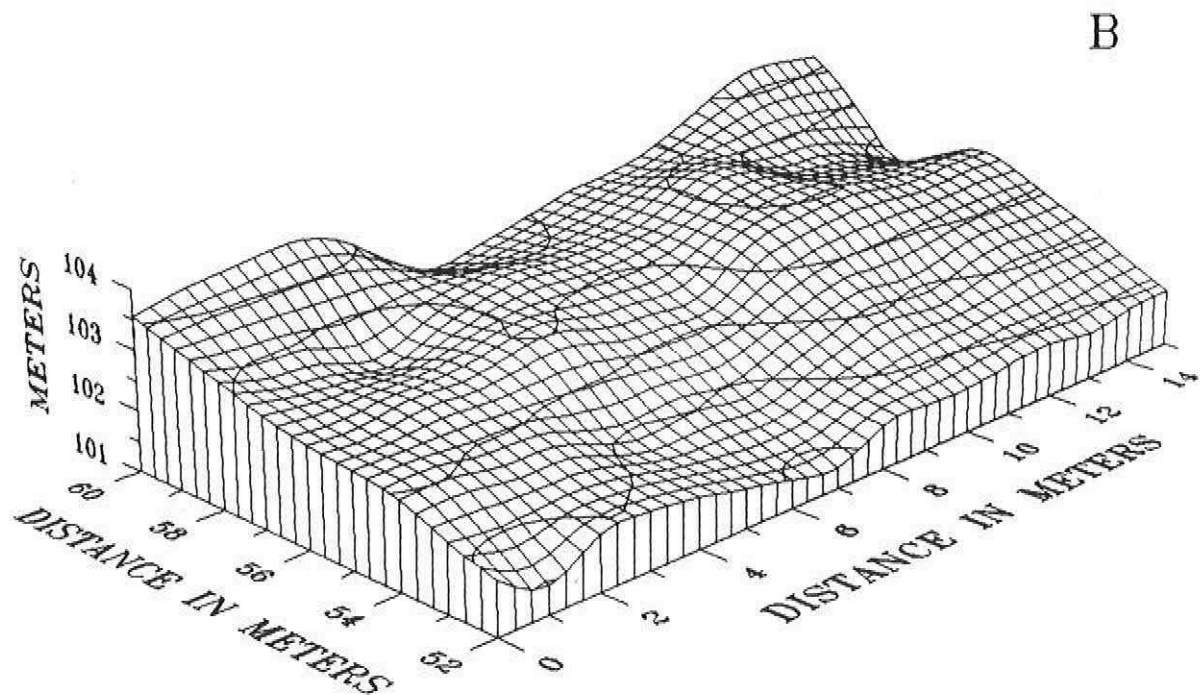
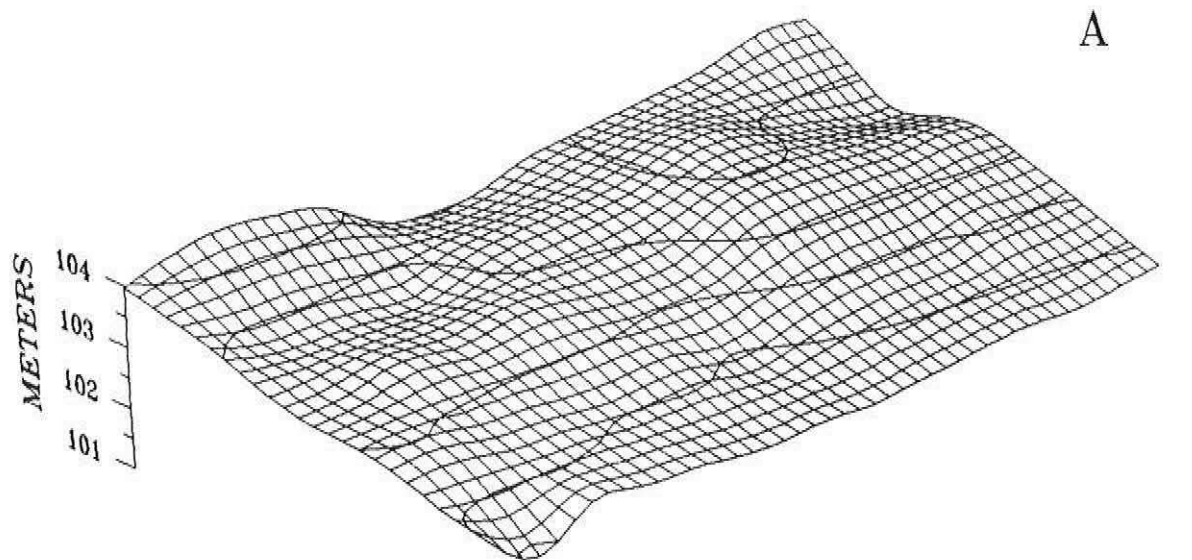
SUBSITE 'B' AT RUSSELL PLACE - RELATIVE TOPOGRAPHY
OF THE SOIL (A) AND BEDROCK (B) SURFACES.



SUBSITE 'B' AT RUSSELL PLACE - RELATIVE TOPOGRAPHY
OF SOIL SURFACE (A) AND DEPTH TO BEDROCK (B)
CONTOUR INTERVAL = 0.2 M



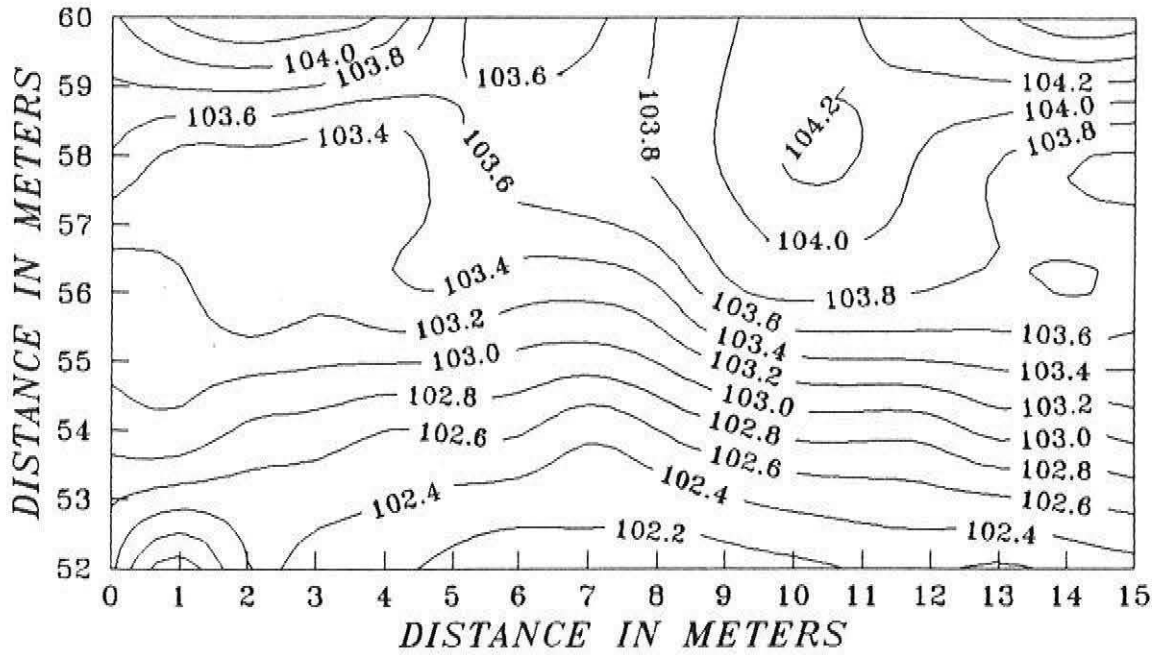
SUBSITE 'A' AT TRINITY SITE - RELATIVE TOPOGRAPHY OF THE SOIL (A) AND BEDROCK (B) SURFACES.



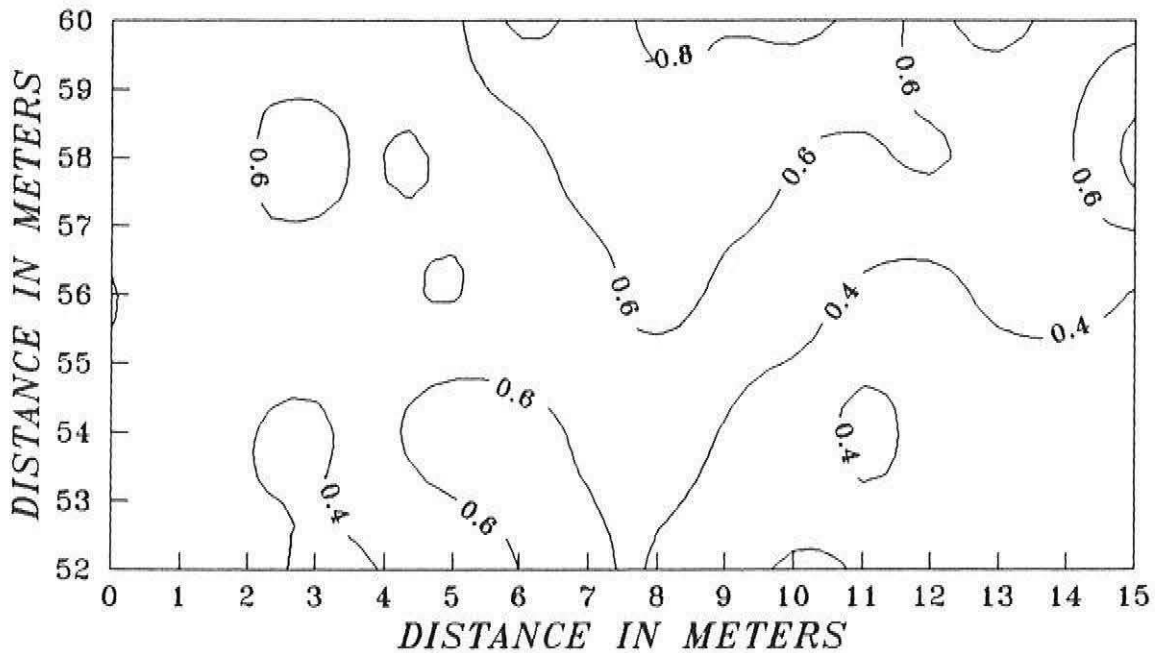
SUBSITE 'A' AT TRINITY SITE
 RELATIVE TOPOGRAPHY OF SOIL SURFACE (A) AND
 DEPTH TO BEDROCK (B)

CONTOUR INTERVAL = 0.2 M

A

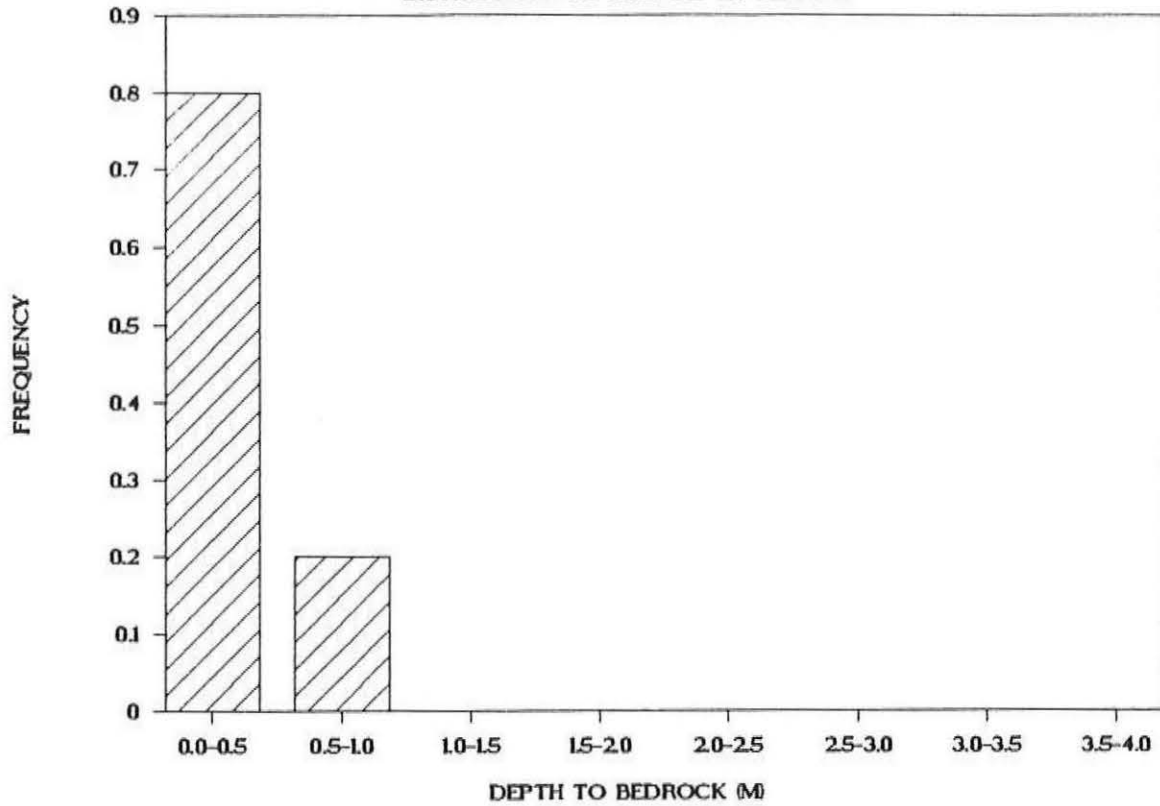


B



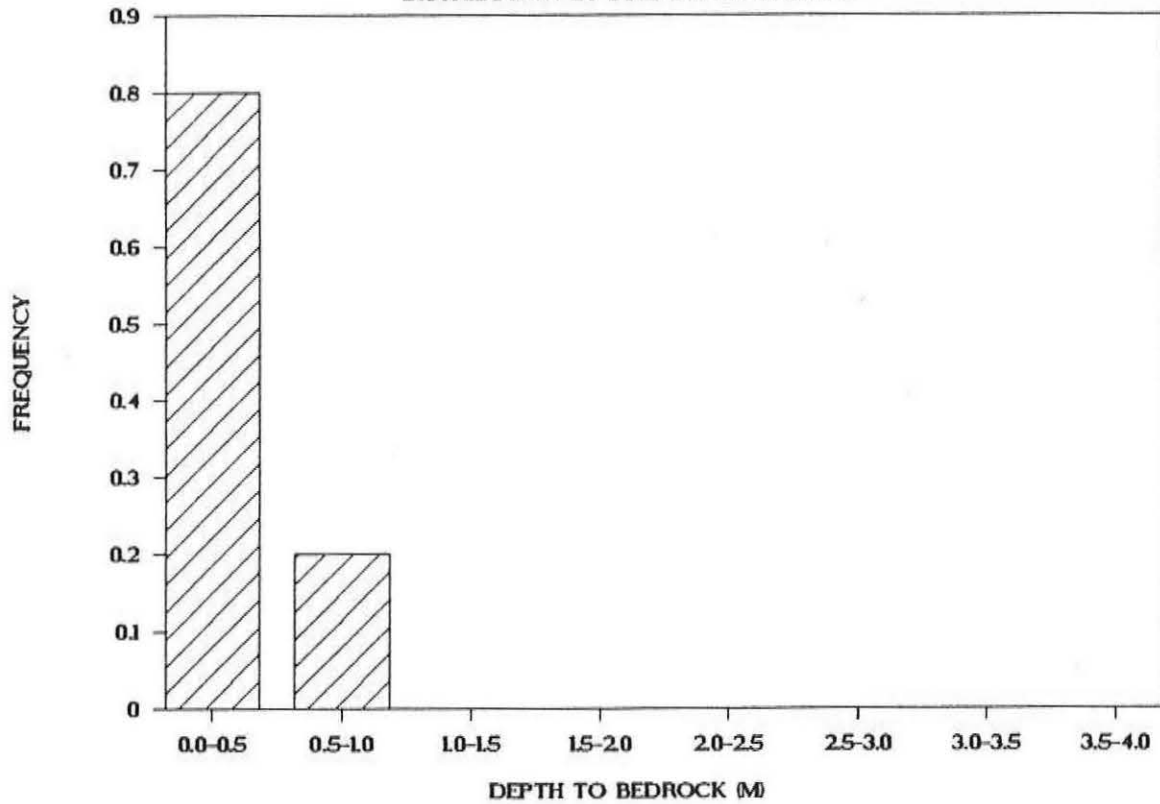
SUBSITE A - TRINITY SITE

DISTRIBUTION BY SOIL-DEPTH CLASSES

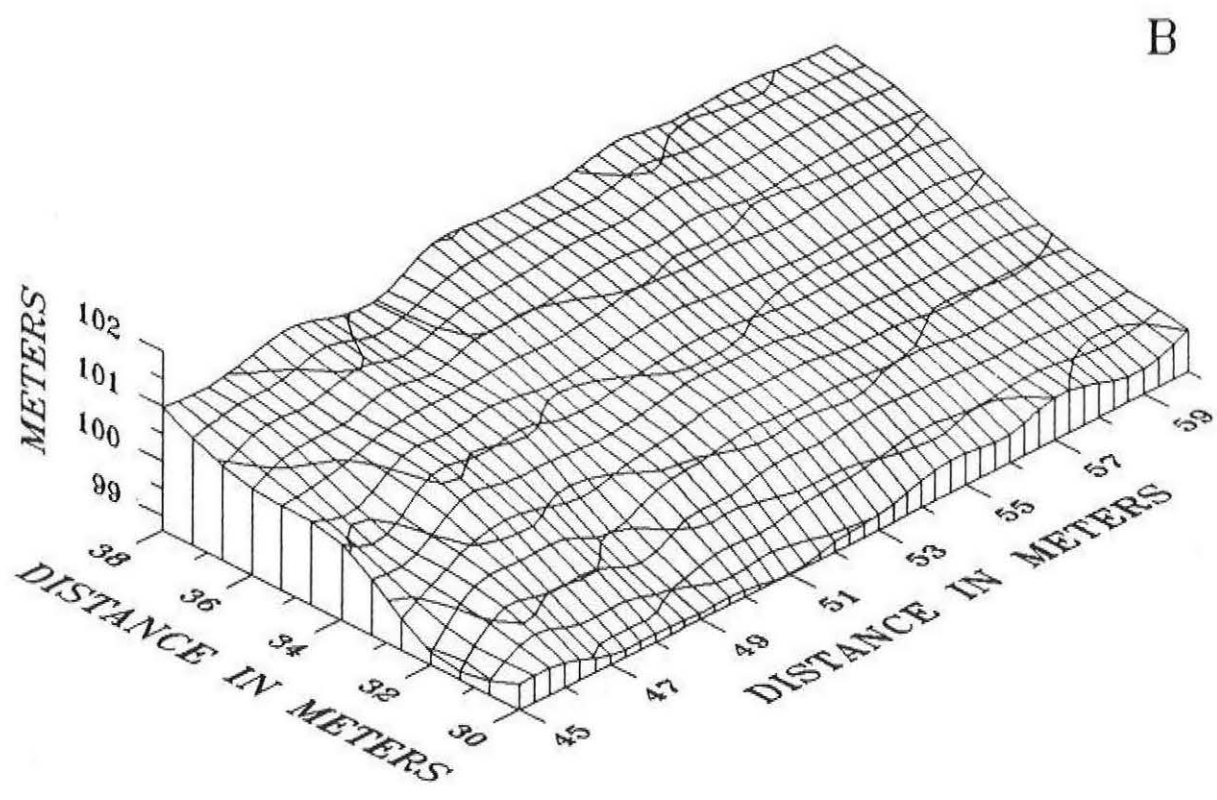
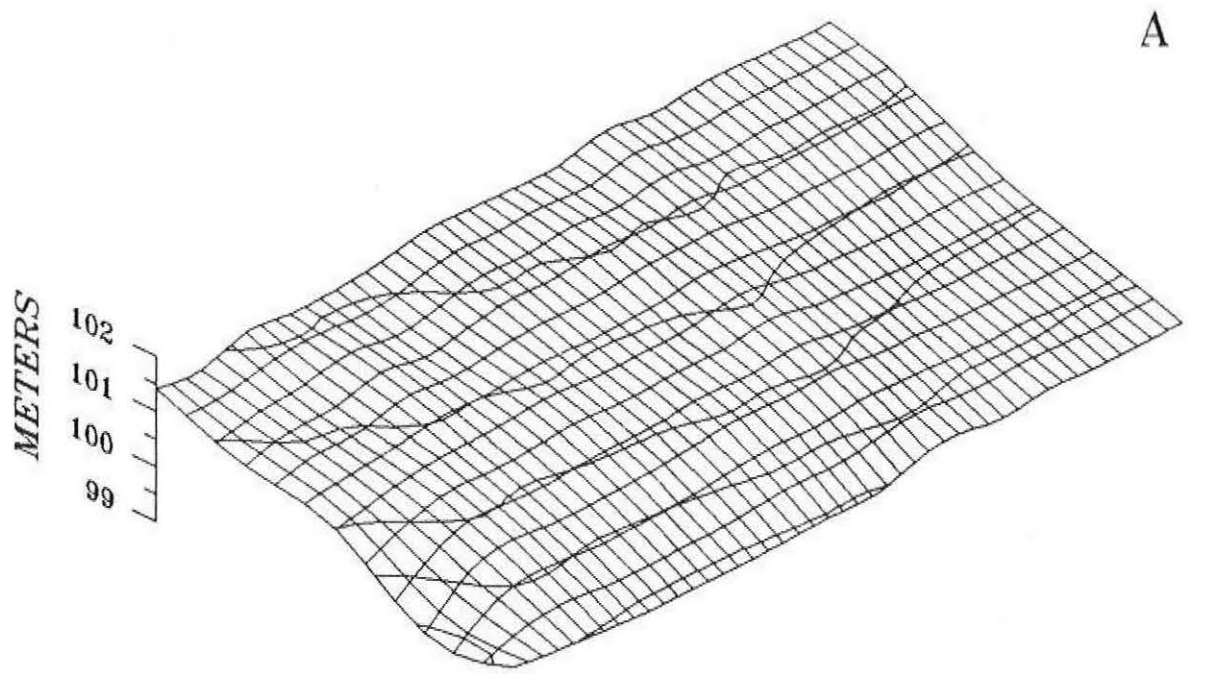


SUBSITE B - TRINITY SITE

DISTRIBUTION BY SOIL-DEPTH CLASSES



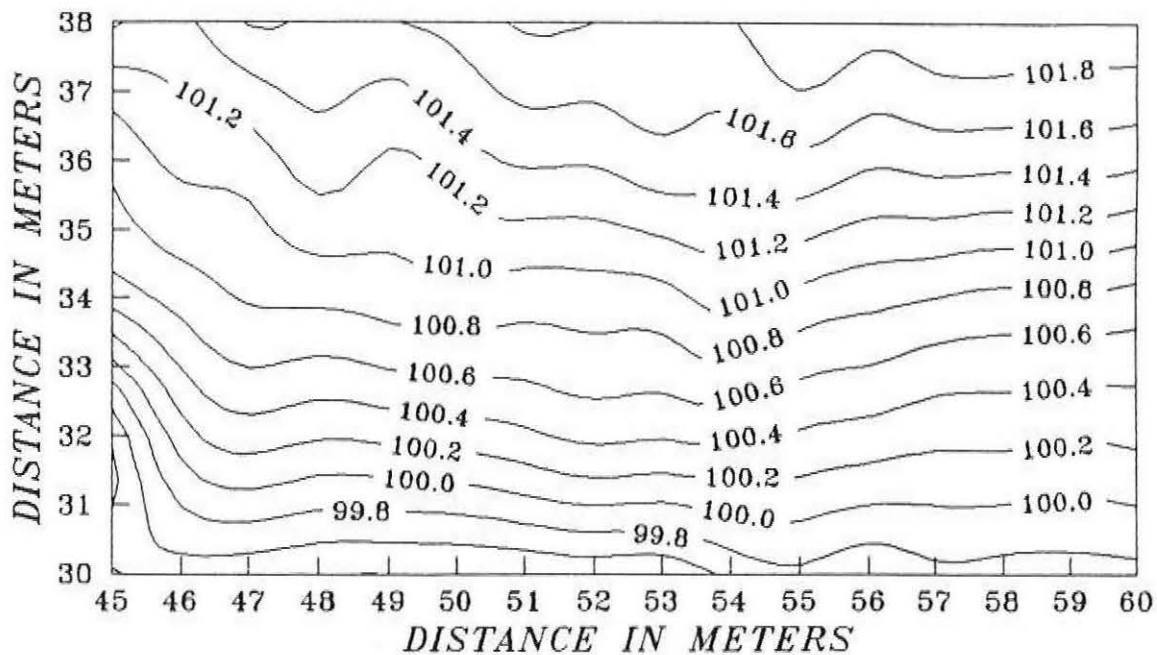
SUBSITE 'B' AT TRINITY SITE - RELATIVE TOPOGRAPHY OF THE SOIL (A) AND BEDROCK (B) SURFACES.



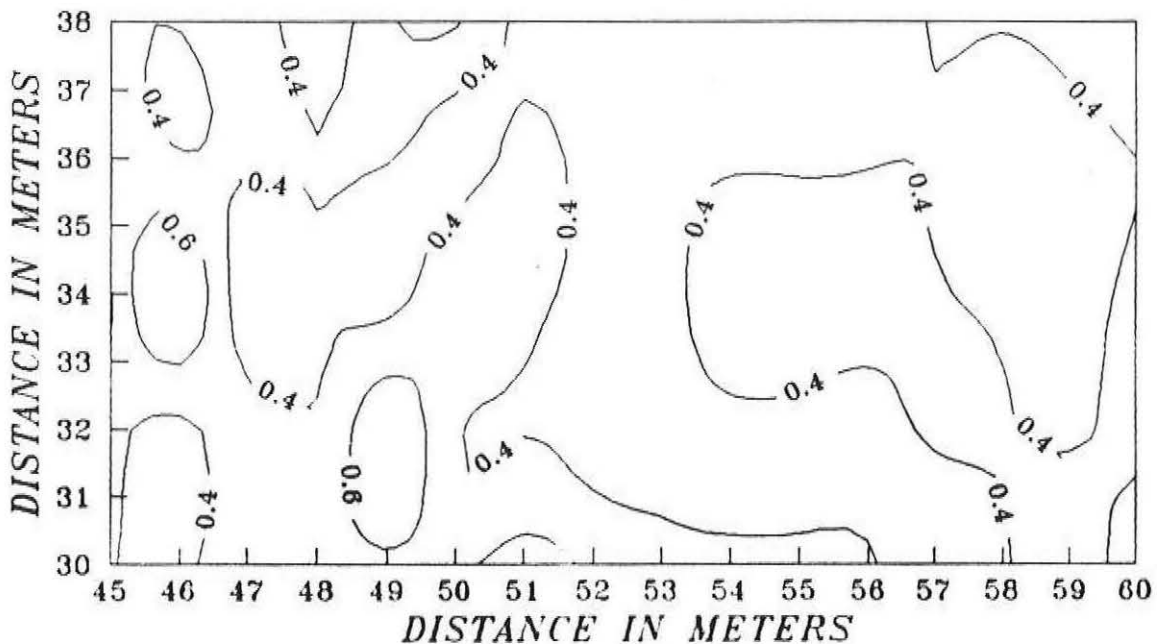
SUBSITE 'B' AT TRINITY SITE
 RELATIVE TOPOGRAPHY OF SOIL SURFACE (A) AND
 DEPTH TO BEDROCK (B)

CONTOUR INTERVAL = 0.2 M

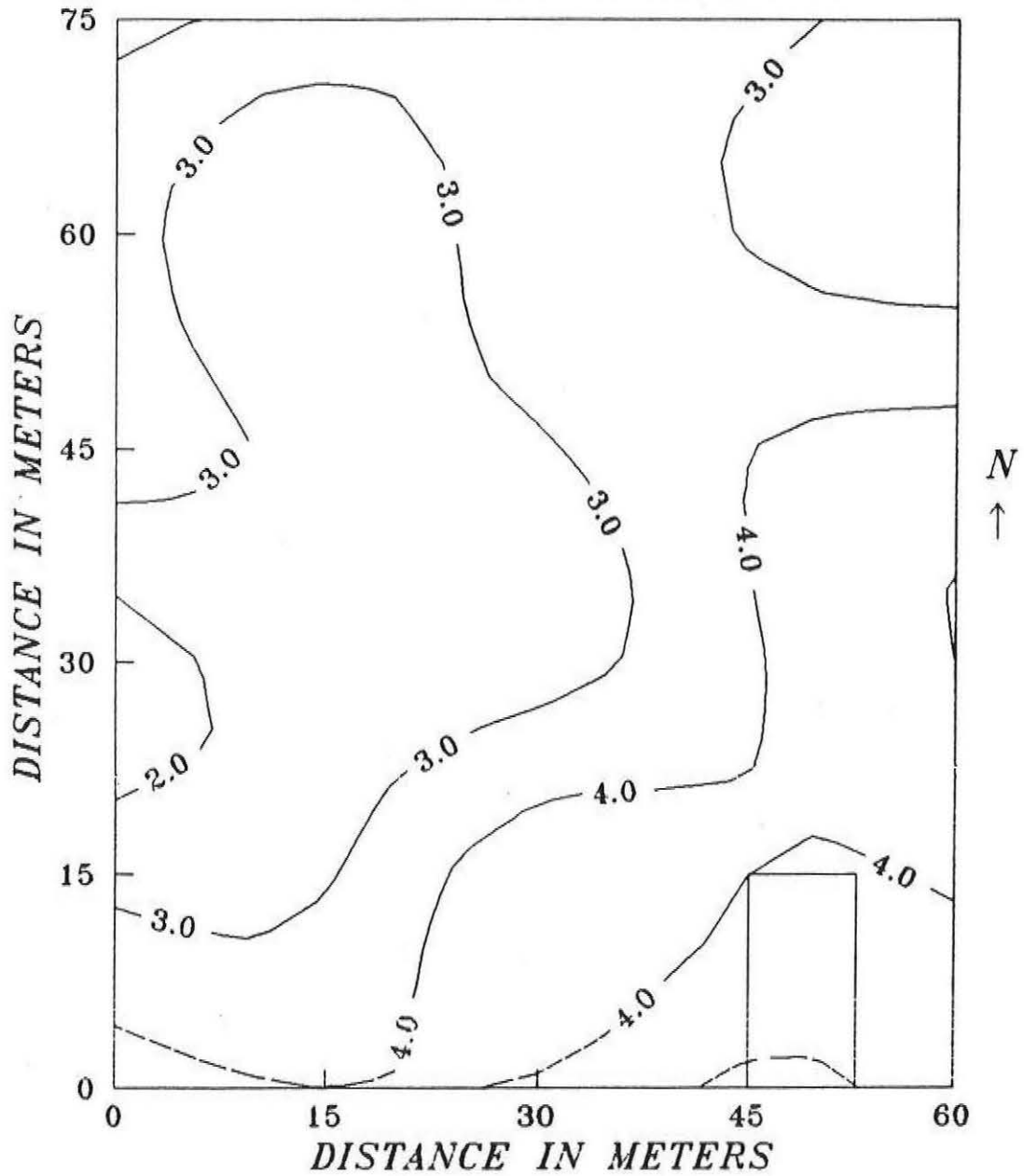
A



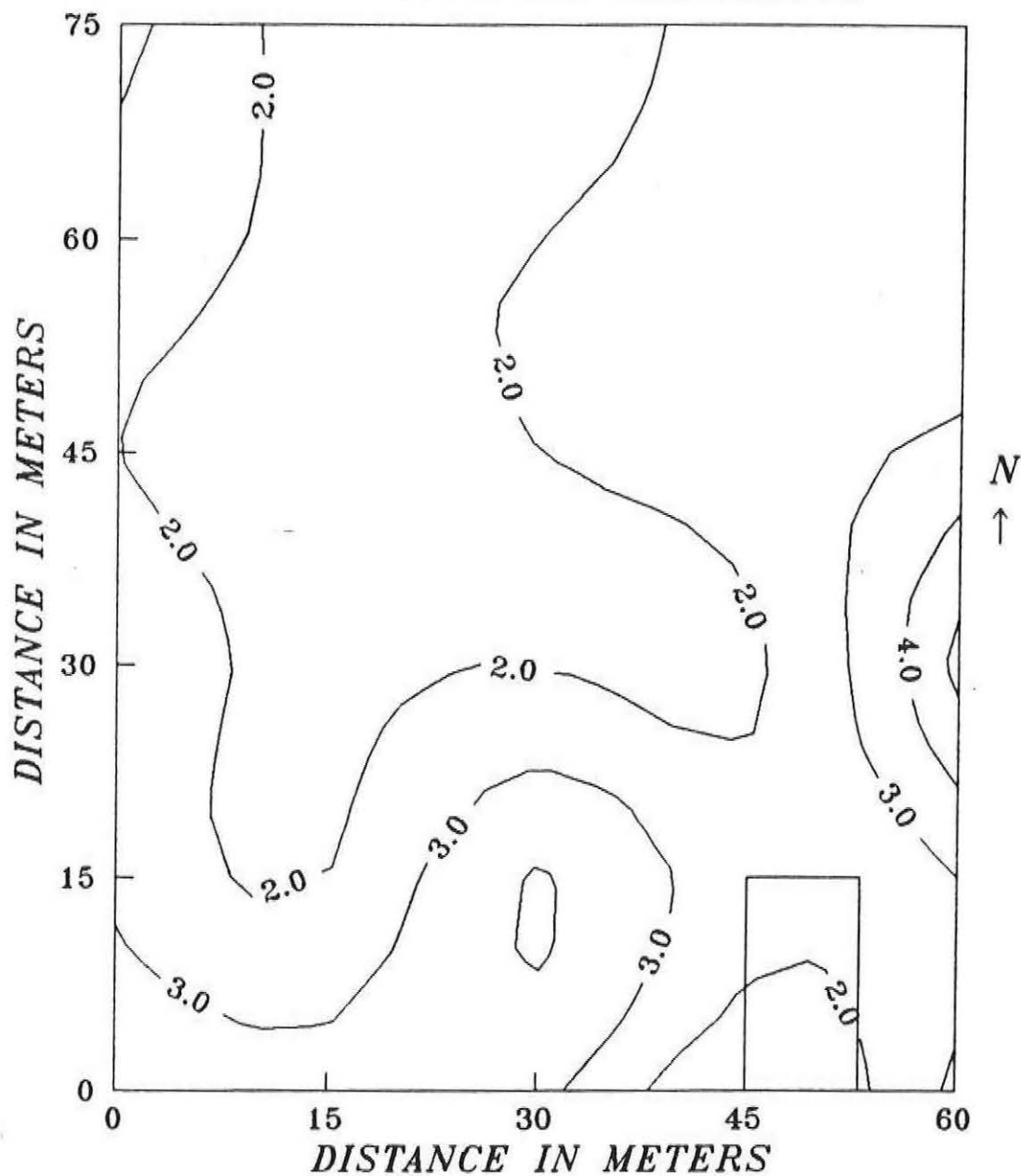
B



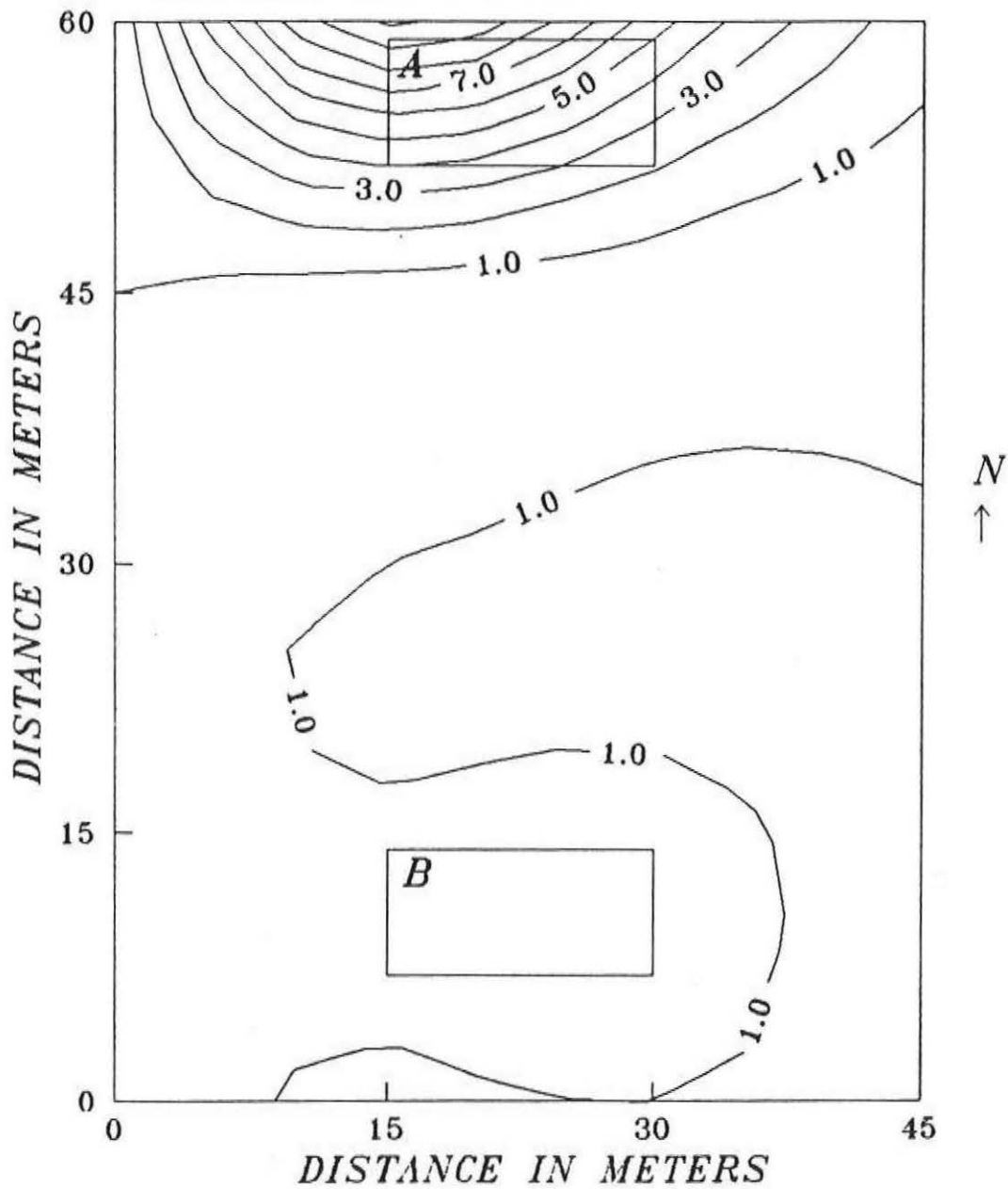
EM38 SURVEY OF BATTERSEA SITE
HORIZONTAL DIPOLE ORIENTATION



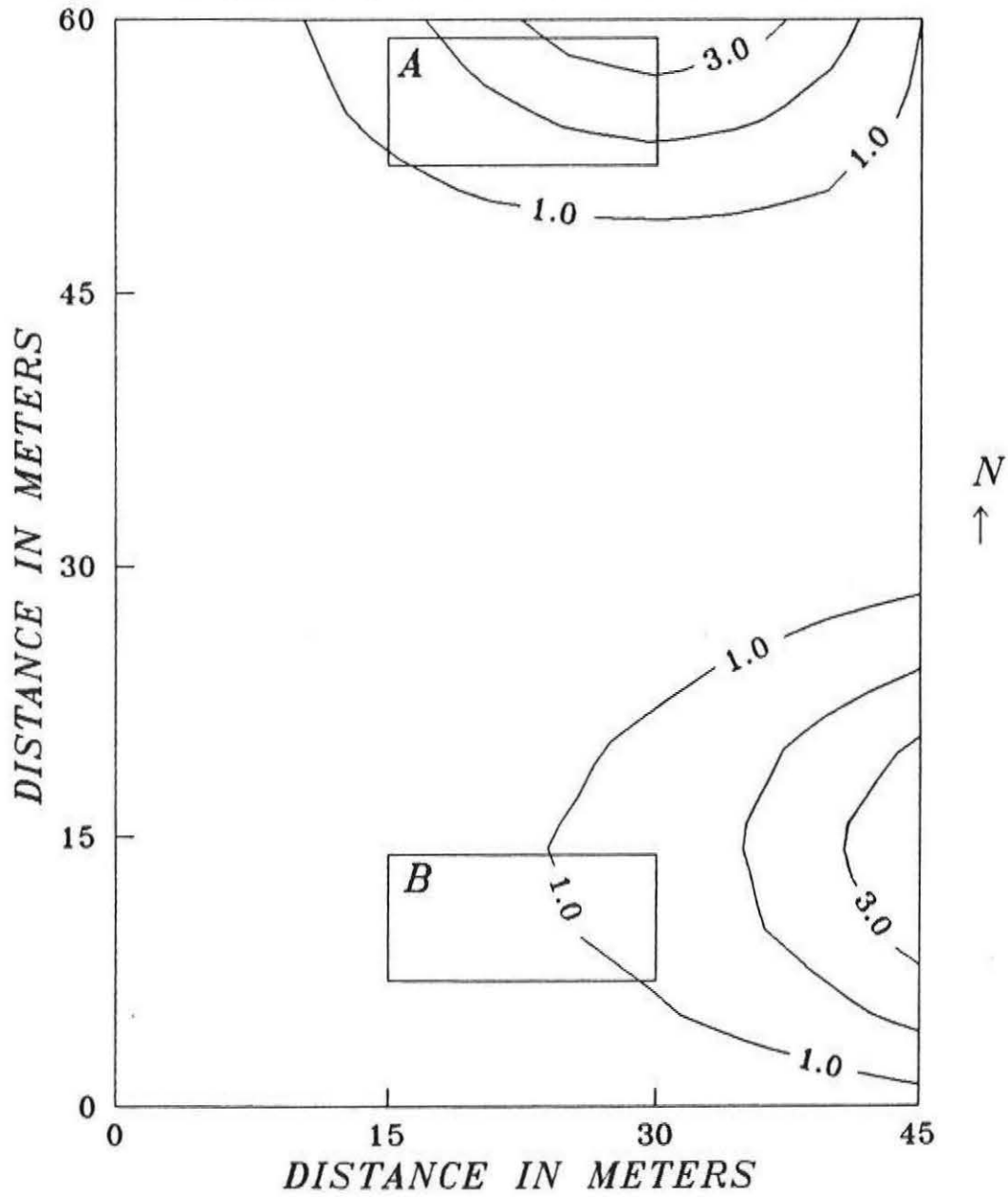
EM38 SURVEY OF BATTERSEA SITE
VERTICAL DIPOLE ORIENTATION



EM38 SURVEY OF MARTIN HILL SITE
 HORIZONTAL DIPOLE ORIENTATION

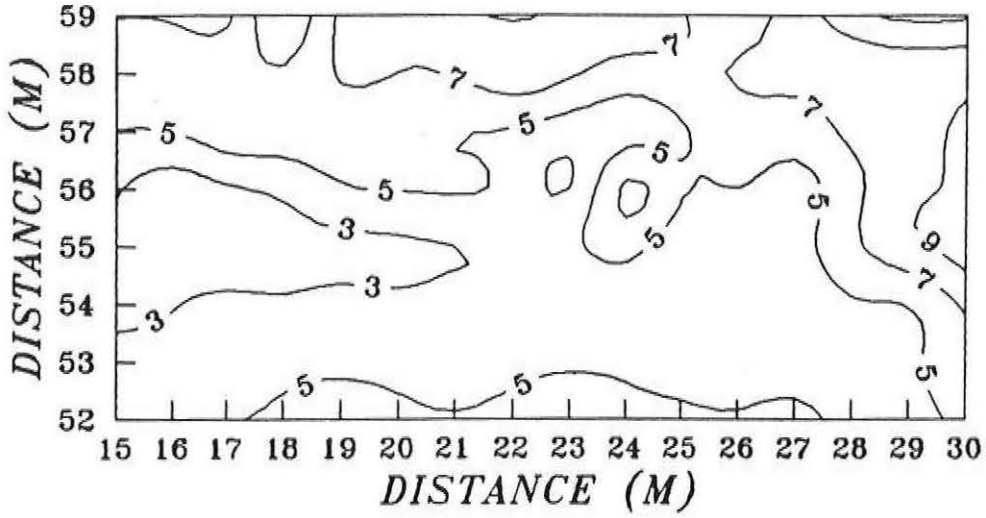


EM38 SURVEY OF MARTIN HILL SITE
VERTICAL DIPOLE ORIENTATION

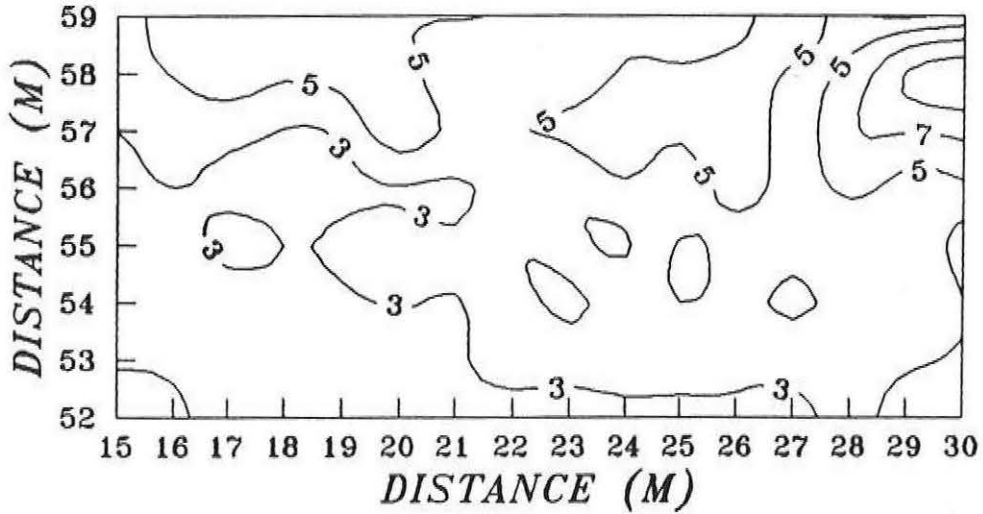


EM38 SURVEY OF SUBSITE A AT MARTIN HILL SITE

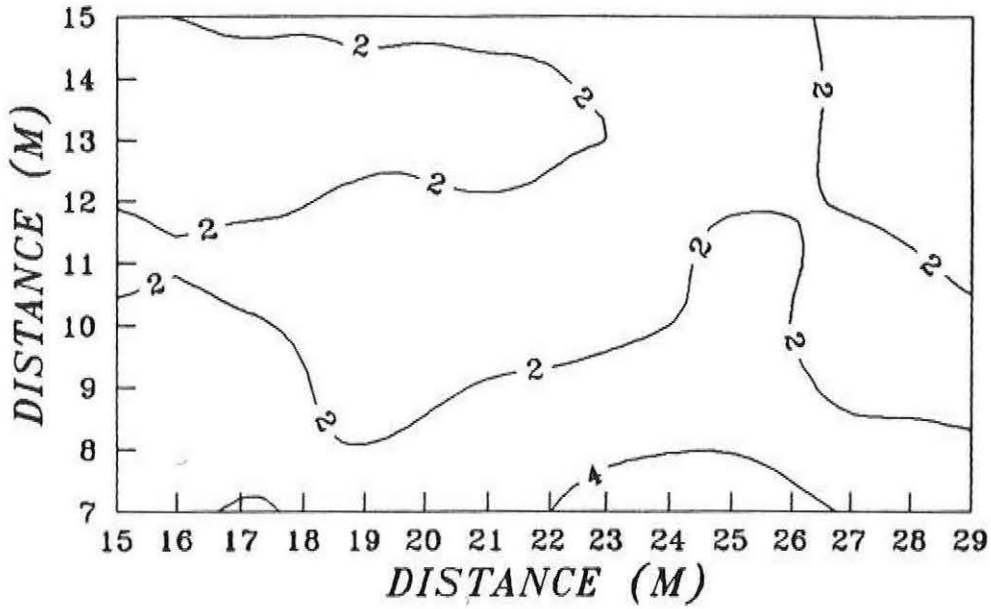
HORIZONTAL DIPOLE ORIENTATION



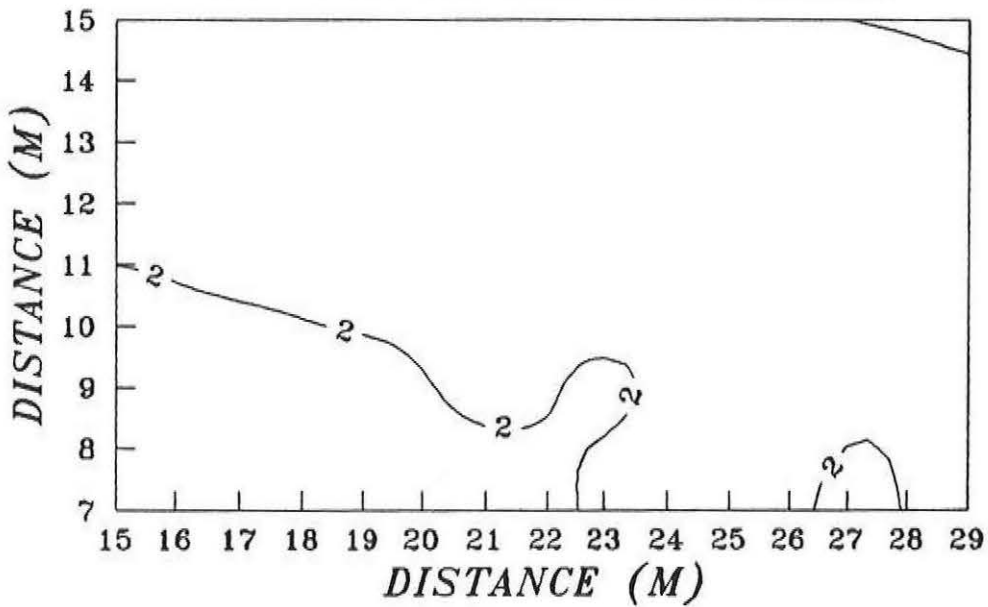
VERTICAL DIPOLE ORIENTATION



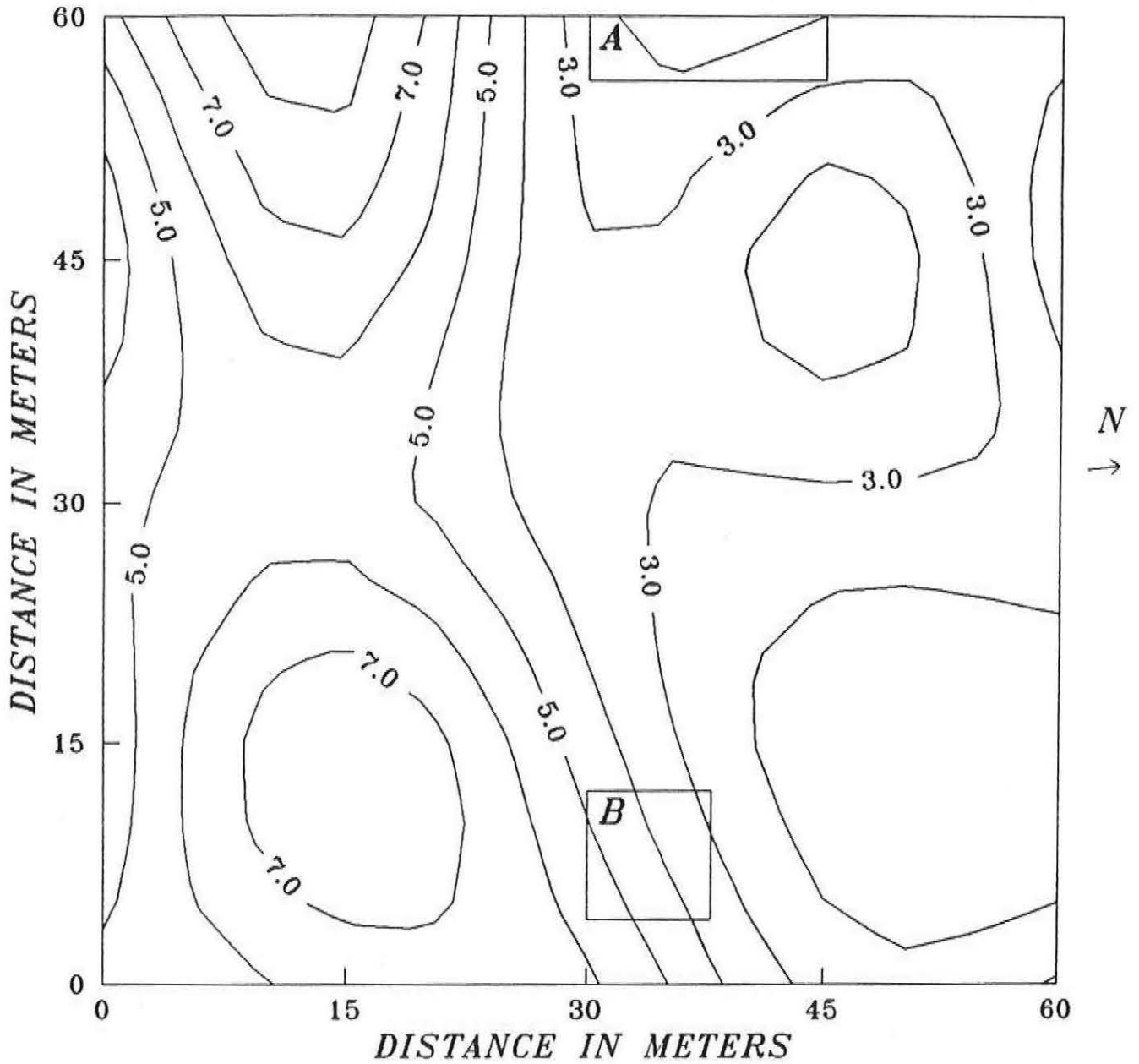
EM38 SURVEY OF SUBSITE B AT MARTIN HILL SITE
 HORIZONTAL DIPOLE ORIENTATION



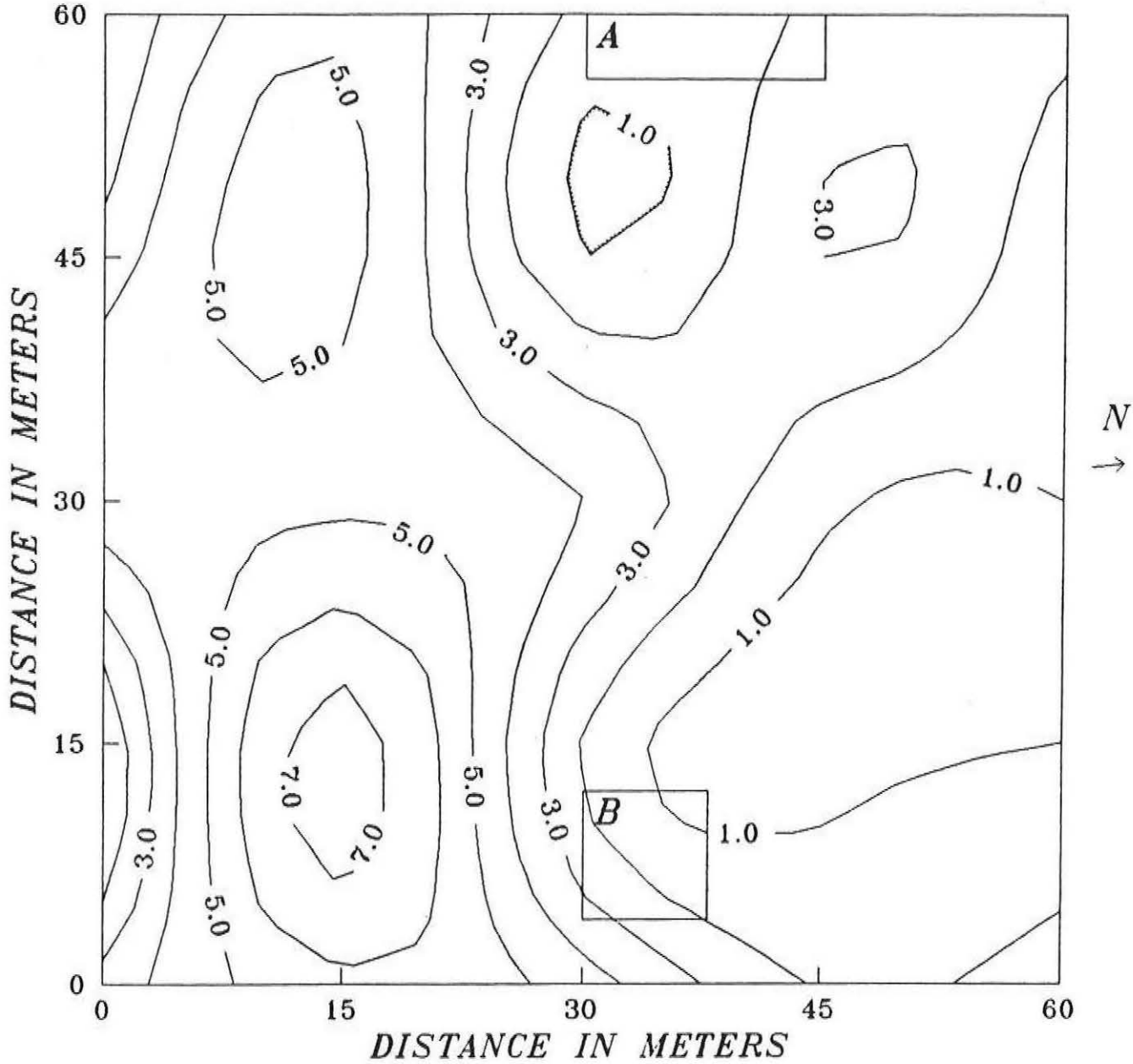
VERTICAL DIPOLE ORIENTATION



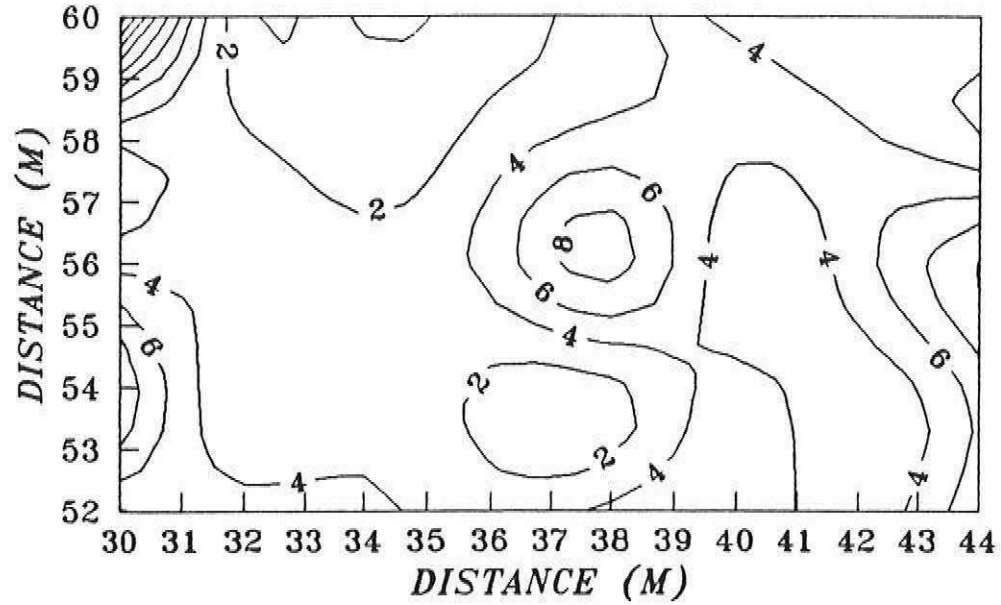
EM38 SURVEY OF RUSSELL PLACE SITE
HORIZONTAL DIPOLE ORIENTATION



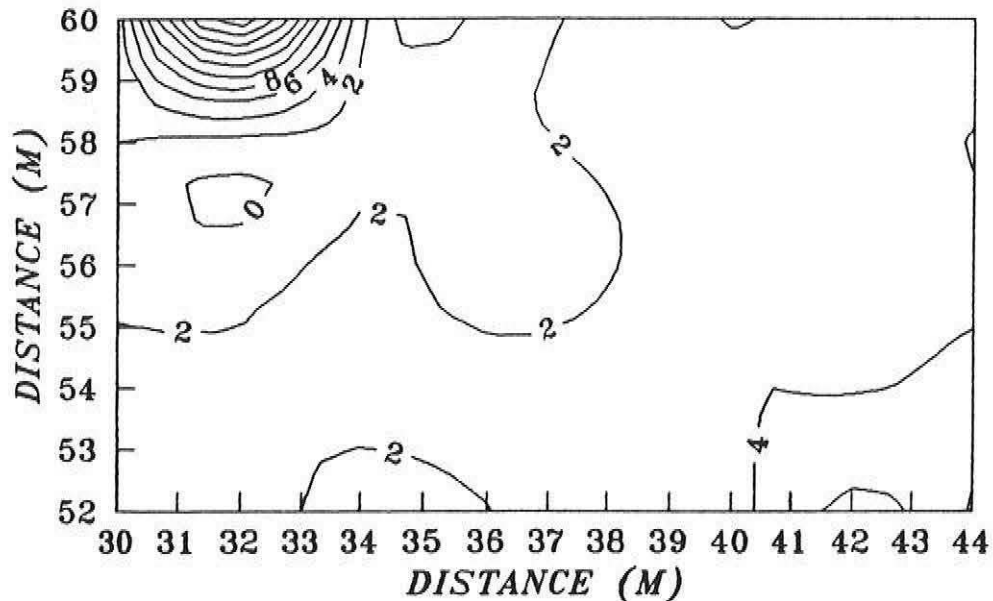
EM38 SURVEY OF RUSSELL PLACE SITE
VERTICAL DIPOLE ORIENTATION



EM38 SURVEY OF SUBSITE A AT RUSSELL PLACE
HORIZONTAL DIPOLE ORIENTATION

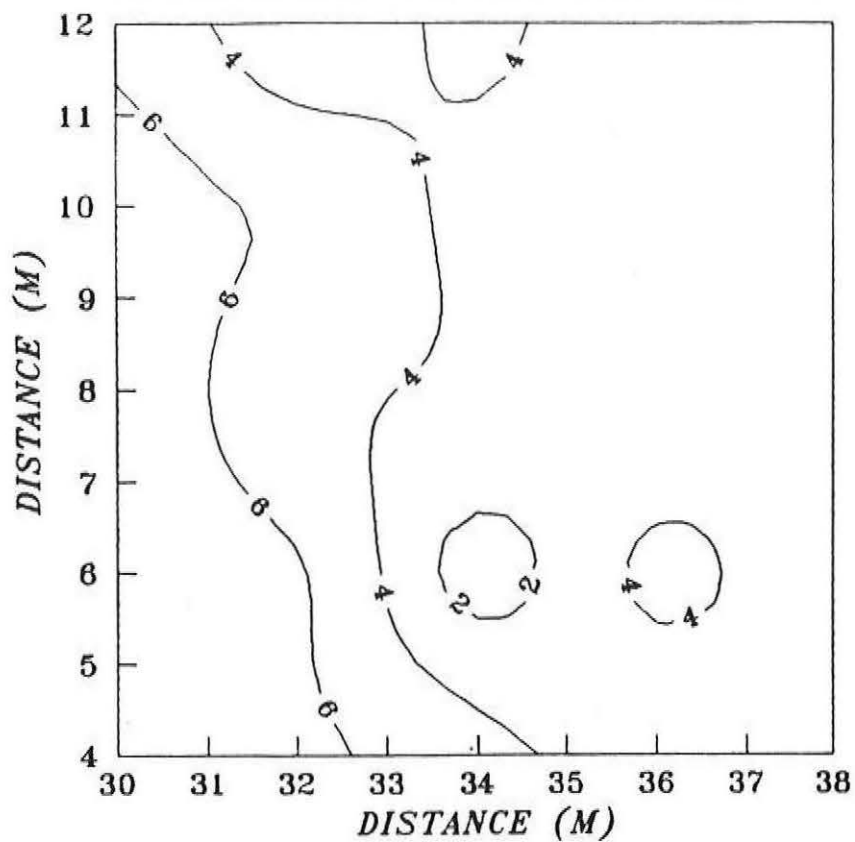


VERTICAL DIPOLE ORIENTATION

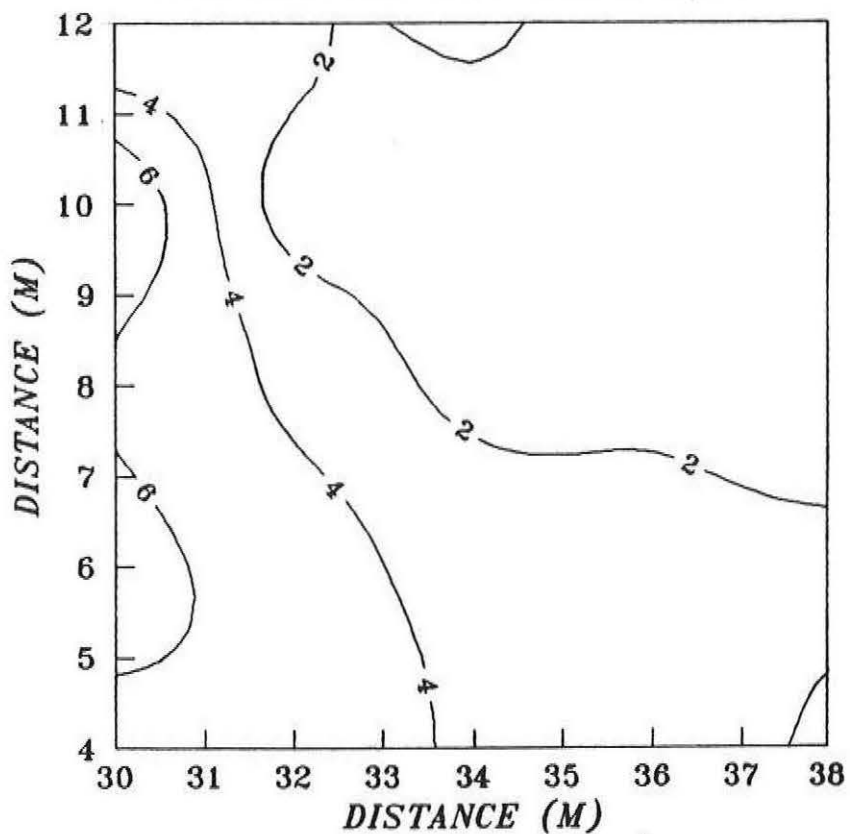


EM38 SURVEY OF SUBSITE B AT RUSSELL PLACE

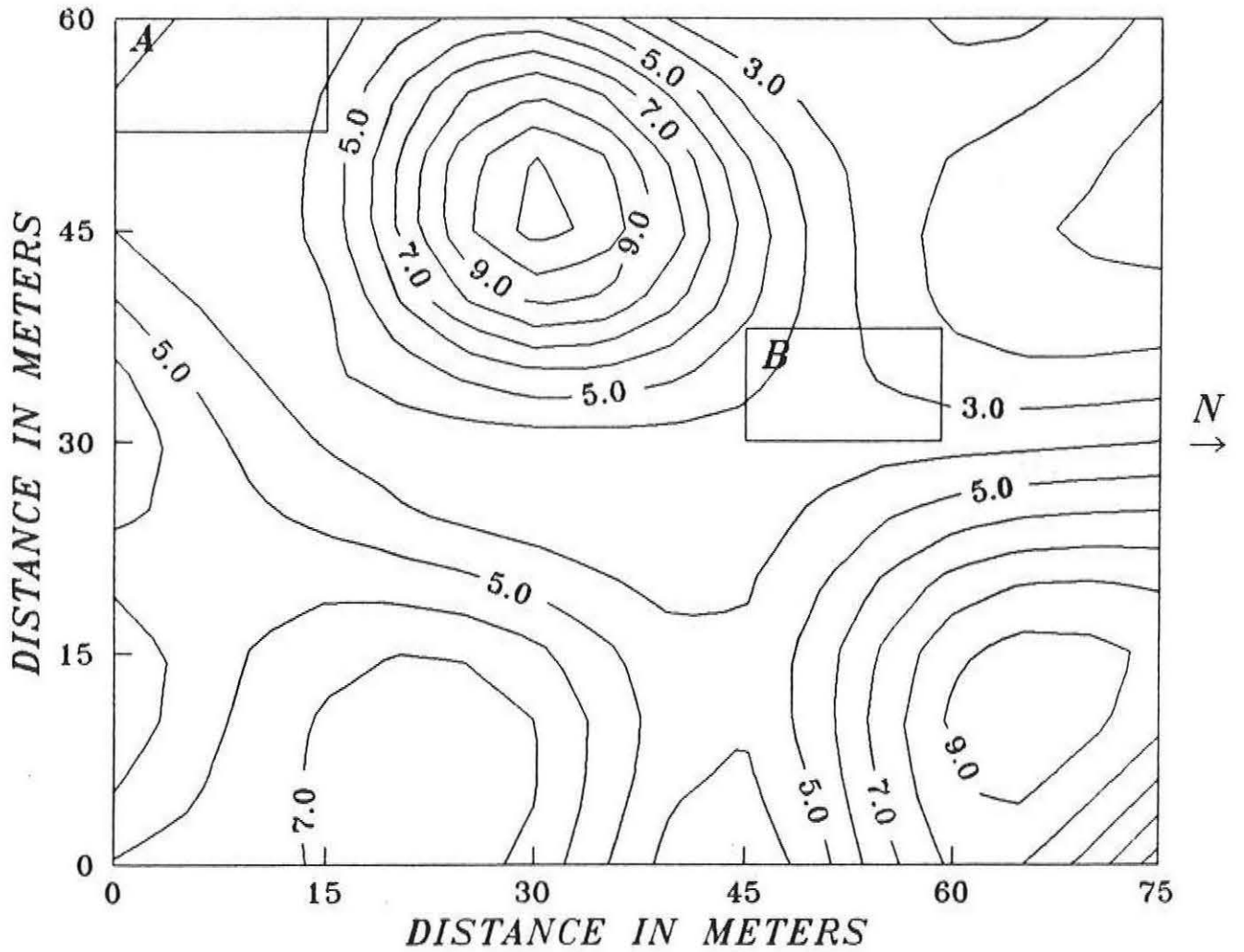
HORIZONTAL DIPOLE ORIENTATION



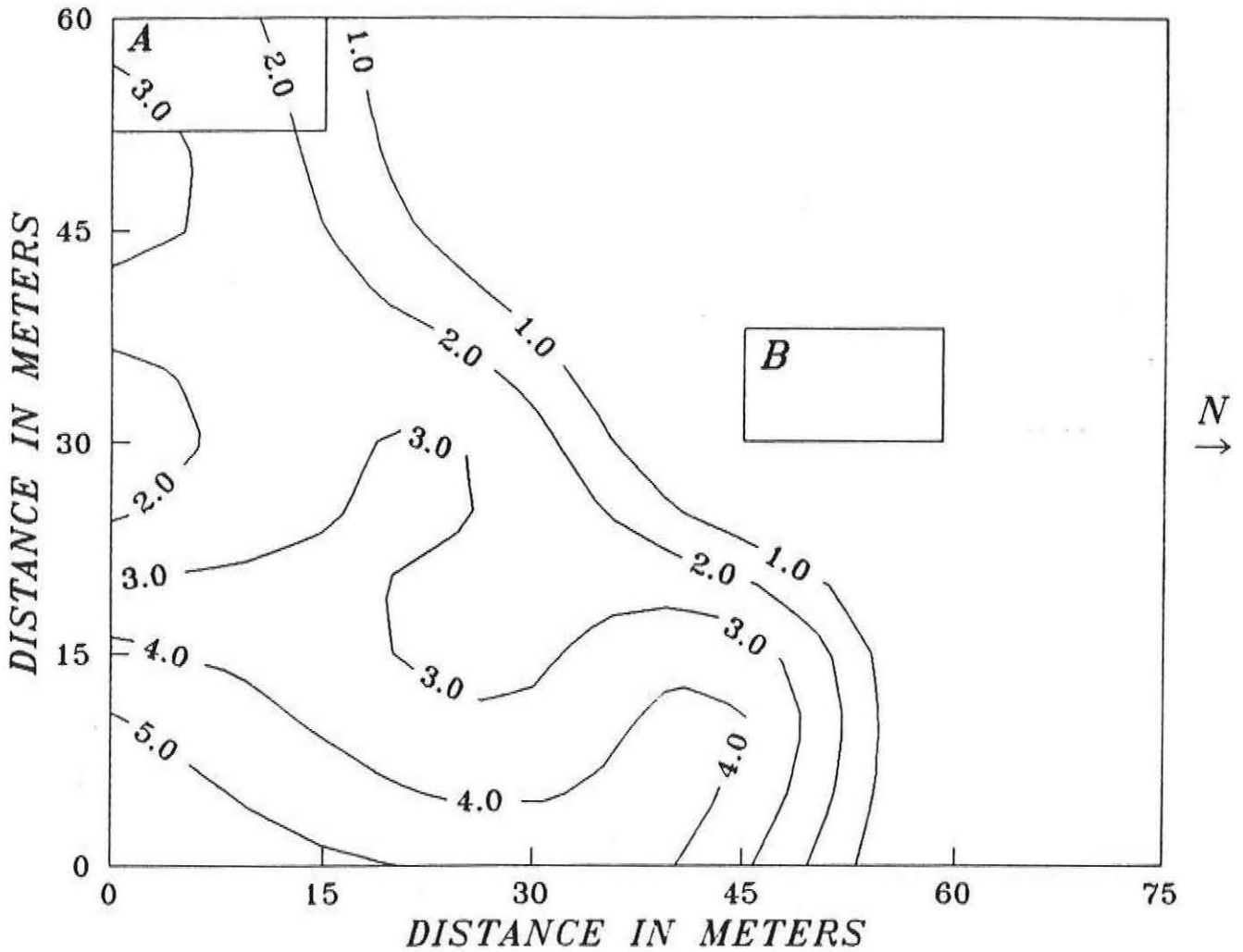
VERTICAL DIPOLE ORIENTATION



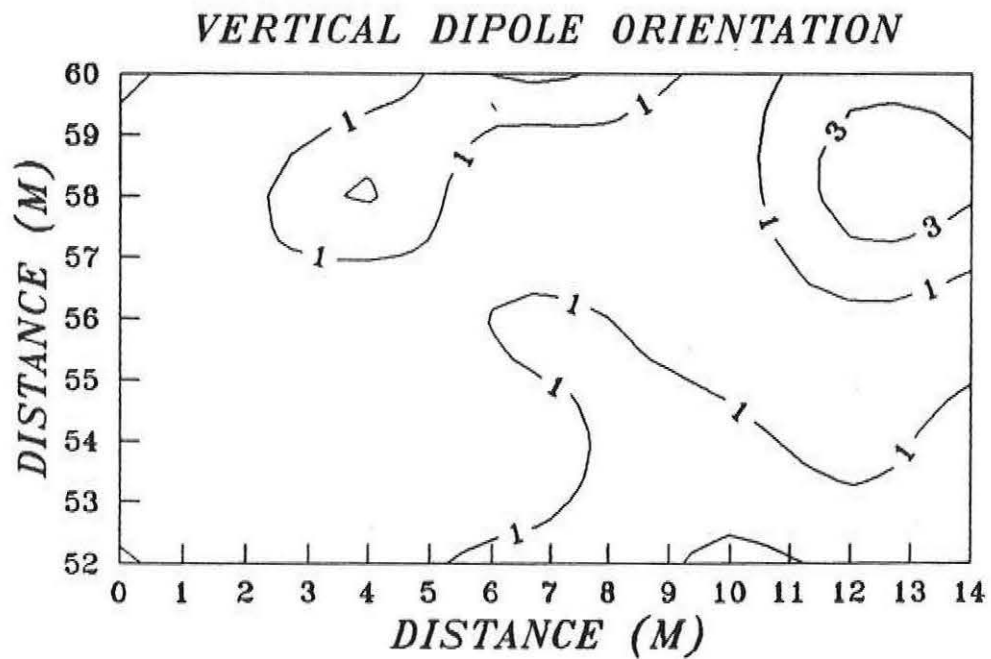
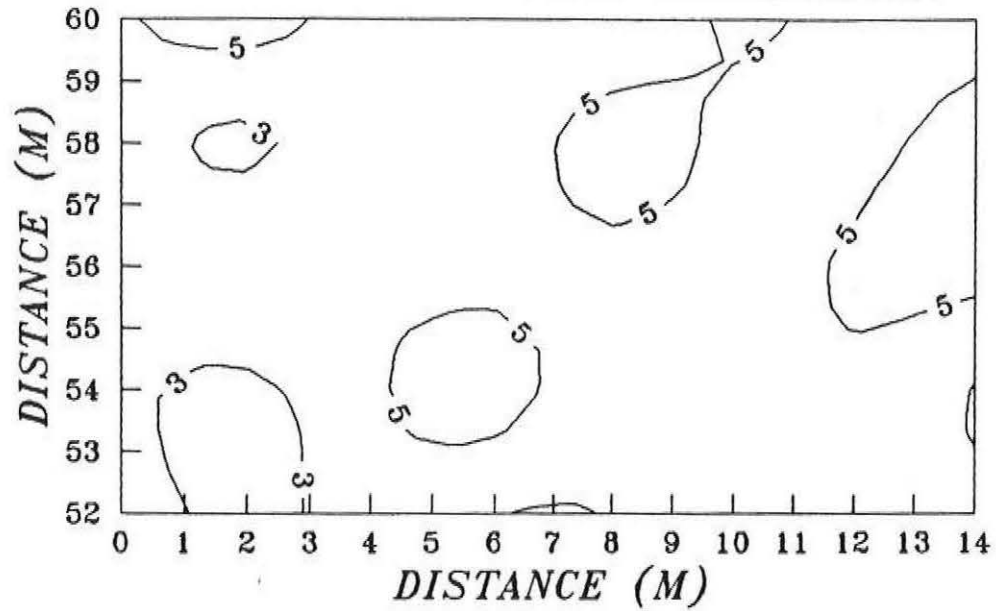
EM38 SURVEY OF TRINITY SITE
HORIZONTAL DIPOLE ORIENTATION



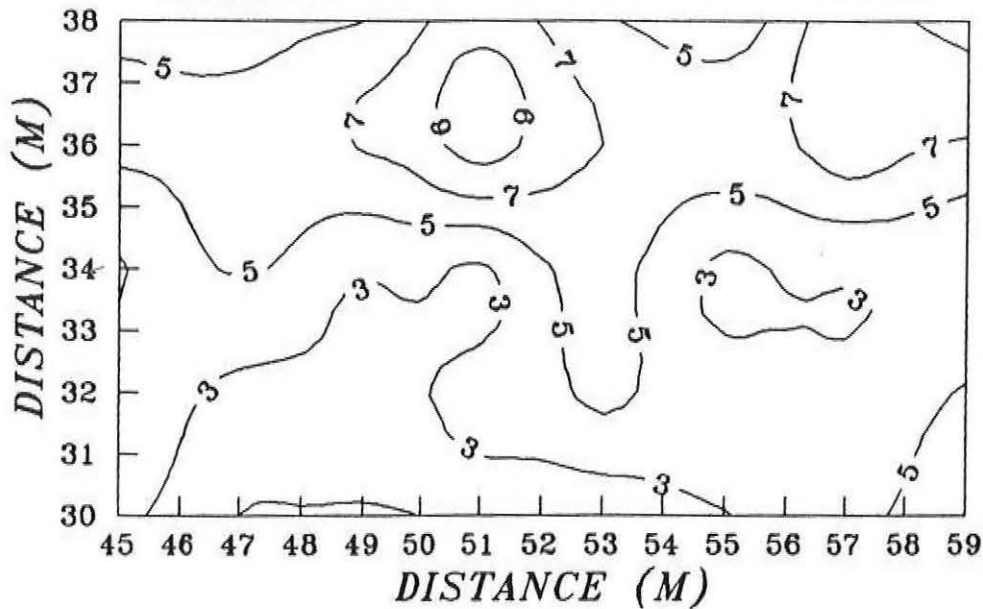
EM38 SURVEY OF TRINITY SITE
VERTICAL DIPOLE ORIENTATION



EM38 SURVEY OF SUBSITE A AT TRINITY SITE
HORIZONTAL DIPOLE ORIENTATION



EM38 SURVEY OF SUBSITE B AT TRINITY SITE
 HORIZONTAL DIPOLE ORIENTATION



VERTICAL DIPOLE ORIENTATION

